Progress in Oceanography 195 (2021) 102593

Contents lists available at ScienceDirect

Progress in Oceanography

journal homepage: www.elsevier.com/locate/pocean

Exploring the future of the Coral Sea micronekton

Aurore Receveur [a,b,c,*], Cyril Dutheil [b,d], Thomas Gorgues [e], Christophe Menkes [b], Matthieu Lengaigne [f], Simon Nicol [a,g], Patrick Lehodey [a,h], Valerie Allain [a], Frederic Menard [c], Anne Lebourges-Dhaussy [i]

[a] OFP/FEMA, Pacific Community, 95 Promenade Roger Laroque, BP D5, Nouméa, New Caledonia
[b] ENTROPIE, UMR 9220, IRD, Univ. de la Réunion, CNRS, 101 Promenade Roger Laroque, Nouméa, New Caledonia
[c] Aix Marseille Univ, Université de Toulon, CNRS, IRD, MIO, Marseille, France
[d] Department of Physical Oceanography and Instrumentation, IOW, Leibniz Institute for Baltic Sea Research Warnemünde, Rostock, Germany
[e] Univ. Brest, CNRS, Ifremer, IRD, Laboratoire d'Océanographie Physique et Spatiale (LOPS), IUEM, F-29280, Plouzane, France
[f] MARBEC, University of Montpellier, CNRS, IFREMER, IRD, Sete, France
[g] Institute for Applied Ecology, University of Canberra, Bruce 2601, Australia
[h] CLS, Sustainable Fisheries, Marine Ecosystem Modelling, 11 rue Hermes, Ramonville, France
[i] IRD, Univ. Brest, CNRS, Ifremer, LEMAR, Campus Ifremer, BP70, Plouzane, France

ARTICLE INFO

Keywords:
Micronekton
Echosounder
Coral Sea
Climate change
Dynamical ecosystem model
Statistical ecosystem model

ABSTRACT

Ecosystem models forced by future climate simulations outputs from the Coupled Model Intercomparison Project Phase 5 (CMIP5) simulate a substantial decline of tropical marine animal biomass over the course of the 21st century. Regional projections are however far more uncertain because of well-known biases common to most CMIP5 historical simulations that propagate within the food web. Moreover, the model outputs for high trophic levels marine fauna suffer from lack of validation based on *in situ* data. In this study, we implement a "bias-mitigation" strategy to reduce the physical oceanography and biogeochemical biases simulated by three CMIP5 models under the future RCP8.5 scenario. We force two very different micronekton models with these "bias-mitigated" outputs to infer the future micronekton changes in the Coral Sea: a 3-D deterministic population dynamics model; and a 3-D statistical model based on *in situ* hydro-acoustic data. These two models forecast a consistent pattern of micronekton abundance changes in the epipelagic layer (0–150 m) by 2100 for three different climate forcing used, with a marked decrease south of 22°S and a smaller increase further north mostly related to temperature and chlorophyll changes. In contrast, changes in the vertical patterns of micronekton predicted by the two models considerably differ in the upper mesopelagic layers (150–450 m) and lower mesopelagic layer (450–1000 m), highlighting the structural sensitivity in model type. Since micronekton are prey of all larger marine predators, those discrepancies in vertical structures of micronekton may hamper our potential to predict how top predators may evolve in the future.

1. Introduction

The range of global biomass estimates for mid-trophic level communities (1–20 cm organisms living between 0 and 1000 m, also called micronekton) is extremely large, with proposed values ranging between 0.5 and 19.5 billion metric tons for migrant mesopelagic organisms alone (e.g., Irigoien et al., 2014; Proud et al., 2017, 2018; Anderson et al., 2019). Micronekton play a central role in the pelagic ecosystem as they constitute food for predators, including commercially targeted species, such as tuna (Bertrand et al., 2002; Duffy et al., 2017; Olson et al., 2014), and emblematic marine species, such as whales and seabirds (Lambert et al., 2014; Miller et al., 2018). In addition, this community may represent a potential food resource for human and aquaculture (St. John et al., 2016). Many species of micronekton migrate daily between the surface layer (0–200 m) during night-time when they feed and the mesopelagic layer (200–1000 m) during the daytime, to avoid visual predation (Bianchi and Mislan, 2016; Klevjer et al., 2016). This diel vertical migration (DVM) contributes largely to the downward flux of nutrients and particulate organic matter via respiration and excretion processes (e.g., Ariza et al., 2015; Bianchi

* Corresponding author at: Thuenen Institute of Baltic Sea Fisheries, Rostock, Germany.
E-mail address: aurore.receveur@9online.fr (A. Receveur).

https://doi.org/10.1016/j.pocean.2021.102593
Received 11 January 2021; Received in revised form 15 April 2021; Accepted 22 April 2021
Available online 7 May 2021

et al., 2013; Drazen and Sutton, 2017; Gorgues et al., 2019). Despite some recent efforts (Fig. 1 in Hidalgo and Browman, 2019), knowledge of mid-trophic level fauna is still limited because of the scarcity of observations (e.g., from dedicated scientific cruises) for such a very diverse group of organisms (Duffy et al., 2017; Olivar et al., 2017, Glover et al., 2018; St. John et al., 2016).

In this study, we aimed at exploring future changes of mid-trophic levels organisms in the Coral Sea, covering more than 4 700 000 km^2 in the southwest Pacific (Ceccarelli et al., 2013). The ecosystem of the Coral Sea exhibits large richness of micronektonic species (e.g., Allain et al., 2012; Olson et al., 2014; Williams et al., 2014; Young et al., 2010) as well as top predators: cetaceans (Mannocci et al., 2014), sharks (Boussarie et al., 2018) and seabirds (Weimerskirch et al., 2017). This ecosystem, referred to as the Archipelagic Deep Basins Longhurst region (Le Borgne et al., 2011; Longhurst, 2007) is expected to have low and moderate vulnerability to climate change in 2035 and in 2100, respectively (Bell et al., 2013). However, the uncertainties around these projections have not been ascertained and predicting the fate of micronekton has not been examined in the region. Moreover, an important effort to collect *in situ* data on micronecton was done since 2011 in the region, that opened opportunity to decrease the incertitude concerning the future of the micronekton.

The future response of the marine food web to anthropogenic forcing largely relies on projections performed with ecosystem models forced by outputs from global climate simulations (Barange et al., 2014; Blanchard et al., 2012; Bryndum-Buchholz et al., 2019; Cheung et al., 2010). Most of these studies project a decrease of marine animal biomass at low and mid-latitudes in response to a declining primary production associated with predicted climate changes (Bopp et al., 2013). However, only a few studies have specifically discussed the evolution of mid-trophic levels organisms in response to these changes (Bryndum-Buchholz et al., 2019; Cheung et al., 2016a; Kwiatkowski et al., 2019; Lotze et al., 2019). For instance, Lefort et al. (2015) predicted a decrease of growth rate and maximum size of micronekton species, with the largest decrease for epipelagic and mesopelagic communities in the tropical central Pacific, Atlantic and Indian Oceans. While these projections indicate a broad decline in tropical marine animal biomass, the dynamic and biogeochemical simulations exhibit large biases and discrepancies at regional levels that propagate within the food web, resulting in substantial regional uncertainties (Bonan and Doney, 2018; Payne et al., 2016).

Indeed, the oceanic components of the climate models from the Coupled Model Intercomparison Project 5 (hereafter CMIP5, Taylor et al., 2012) display substantial present-day physical and biogeochemical biases in the western Pacific, including a cold tongue that penetrates too far into the western Pacific (e.g. Li et al., 2015). Those biases can propagate into lower and upper trophic levels when coupled to population dynamic models, potentially limiting the reliability of mid-trophic organisms biomass projections (Lehodey et al., 2013; Payne et al., 2016). In addition, projections of the future oceanic physical and biogeochemical states also differ depending on the model considered. Here, we develop a "bias-mitigation" strategy to minimize the climatological biases of the coupled CMIP5 models while keeping the inter-model diversity through dedicated ocean biogeochemical model experiments. These latter are forced by observationally derived boundary conditions onto which future anomalous atmospheric changes computed from three CMIP5 models are applied. This strategy, widely applied in atmospheric sciences (e.g., Knutson et al., 2008; Dutheil et al., 2019), has rarely been applied in ocean science (e.g., Matear et al., 2015).

These simulations provide three plausible future oceanic conditions (e.g., temperature, salinity, currents, dissolved oxygen concentration, primary production) for two different types of micronekton models: the Spatial Ecosystem and Population Dynamics Model (SEAPODYM), an end-to-end deterministic ecosystem model that includes a micronekton representation (Delpech et al., 2020; Lehodey et al., 2008; 2010a,b; 2015a,b); and the 3-D statistical model of Receveur et al. (2019), which uses observed acoustic data to relate micronekton vertical distribution to environmental conditions. The use of the different oceanic forcing and ecosystem models allows disentangling the relative importance of oceanic conditions and micronekton models on the uncertainties of future micronekton changes in the Coral Sea.

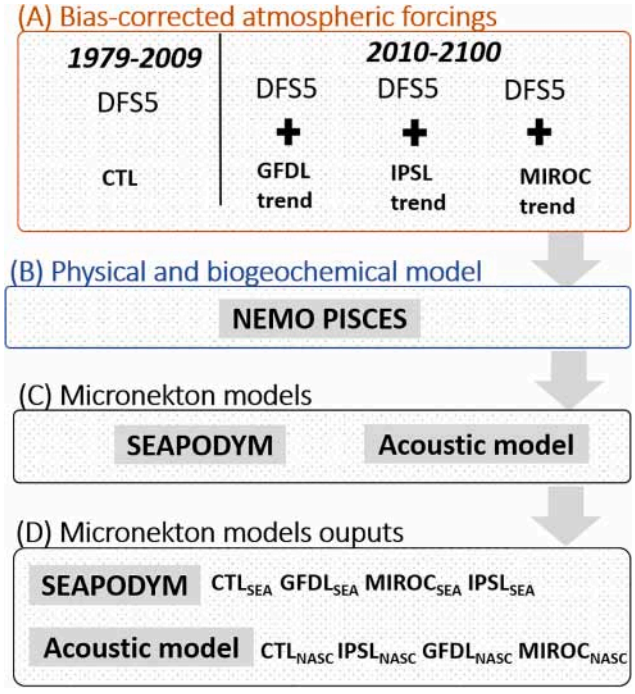

Fig. 1. Modeling framework detailing the combination of atmospheric forcing models (A), physical and biogeochemical oceanographic model (B) and micronekton biological models (C) with their respective outputs (D) used in the analysis. CTL = 'control simulation'; GFDL, IPSL and MIROC acronyms are given in Table 1; SEA = 'SEAPODYM'; NASC = 'Nautical Area Scattering Coefficient'.

2. Material and methods

Physical and biogeochemical inputs necessary to force the two micronekton models were extracted from simulations performed with the NEMO-PISCES ocean biogeochemical model (Fig. 1). This model was forced by atmospheric variables extracted from one reanalysis for the hindcast period (1979–2009) and from the same reanalysis onto which forecast (2010–2100) atmospheric trends computed from the atmospheric outputs of the three CMIP5 climate coupled models were added. The following paragraphs describe in detail each step of this modelling strategy.

2.1. Hindcast and forecast surface atmospheric forcing

For the hindcast period (1979–2009, labelled CTL), the atmospheric fields that are representative of observed variability and used to force the ocean model were derived from an adjusted version of the ERA-interim reanalysis: Drakkar Forcing Sets (DFS5, Dussin et al., 2016) (Fig. 1A).

For the forecast period (2010–2100), the scenario selected was the Representative Concentration Pathway 8.5 (RCP8.5), for which the radiative forcing due to aerosols and greenhouse gases reaches 8.5 W. m^{-2} by 2100 (van Vuuren et al., 2011). However, we did not directly use the surface atmospheric fields from the CMIP5 global coupled climate models to force our ocean biogeochemical model. These global models share prominent biases in their representation of the present-day tropical Pacific climate (e.g., Cai et al., 2015; Brown et al. 2020), which could hamper the reliability of future physical and biogeochemical

projections (e.g., Xie et al., 2015). To avoid including known CMIP5 present-day biases in our surface atmospheric forcing, we developed a method to minimize biases in the atmospheric forcing (referred as "bias-mitigated" method). The method consisted in using, for the forecast period, the same forcing dataset (DFS5) as used for the hindcast period (1979–2009), repeated three times (to cover the 90-years 2010–2100 period: 2010–2039, 2040–2069, 2070–2100), onto which forecast surface forcing anomalies from three selected CMIP5 coupled climate models were added (Fig. 1A). These anomalies were computed relative to the 1979–2009 period for filtered (31-years Hanning filter) zonal and meridional wind stress, air temperature and humidity at 2-m, shortwave and longwave radiations, snowfall and precipitation. The subseasonal to decadal variations of this forecast forcing dataset was hence fully constrained by the reanalysis while the anthropogenic filtered trends over the 2010–2100 period was set to the one projected by each selected CMIP5 model. This method allowed constraining the background state and natural climate variability to remain close to the observations, while applying the low-frequency changes induced by the anthropogenic perturbations derived from CMIP5 models.

To account for the diversity of the regional changes projected by global CMIP5 models, we applied our bias-mitigated strategy using global projections from three different CMIP5 models: the GFDL-ESM2G model (Dunne et al., 2012), the MIROC-ESM model (Watanabe et al., 2011) and the IPSL-CM5-MR model (Dufresne et al., 2013) (Table 1). For simplicity, we referred to our bias-mitigated simulations with each CMIP5 model as GFDL, MIROC and IPSL, respectively.

2.2. Hindcast and forecast physical and biogeochemical ocean states

While most CMIP5 models project relatively consistent oceanic changes in response to warming at a global scale (e.g., for sea surface temperature), these projections are generally far less consistent at regional scales. Such a spread is particularly visible in forecast marine biogeochemical projections (e.g., Bopp et al., 2013; Fu et al., 2016; Kwiatkowski et al., 2017; Moore et al., 2018) and arises from dynamical (Wang et al., 2014) and biogeochemical model differences (Laufkötter et al., 2015). Here, we proposed to use a single ocean-biogeochemical model so that observed differences in a projected micronekton biomasses by one specific micronekton model may be attributed only to differences in the anthropogenic trends derived from the above mentioned CMIP5 models.

The four atmospheric fields (CTL, GFDL, MIROC and IPSL) were used to force the NEMO (Nucleus for European Modelling of the Ocean; Madec, 2008) dynamical ocean model that includes the biogeochemical component PISCES (Pelagic Interaction Scheme for Carbon and Ecosystem Studies; Aumont et al., 2015). PISCES is a Nutrient-Phytoplankton-Zooplankton-Detritus model (Aumont et al., 2015), which explicitly simulates the cycle of five nutrients (nitrate, ammonium, iron, silicate, and phosphate), as well as two types of phytoplankton (nanophytoplankton and diatoms), two sizes of zooplankton (micro- and meso-zooplankton), two sizes of detritus (small and large particulate organic carbon) and dissolved organic carbon. We used the ORCA2 grid configuration, in which the zonal resolution is set to 2°, and meridional resolution ranges from 0.5° at the equator to 2° toward the poles. The model grid is tripolar, with two poles in the Northern Hemisphere (over North America and Siberia) and one centered over Antarctica. The model uses 31 z-levels (ranging from 5 m to 5500 m) in the vertical, with 20 of these levels lying in the upper 500 m. Details about this model configuration can be found in Aumont et al. (2015).

We obtained four ocean simulations of the dynamical and biogeochemical variables necessary to force our two micronekton models: one control simulation (labelled CTL_{NM}, 1979–2009) representative of the hindcast oceanic conditions and three simulations representative of three plausible future oceanic conditions built using our bias-mitigated forcing from the three CMIP5 models (labelled $GFDL_{NM}$, $MIROC_{NM}$ and $IPSL_{NM}$, 2010–2100, Fig. 1B).

The IPSL simulation displayed significant biases over the historical period compared to observations. North of 15°N, surface temperatures were too warm by up to 1 °C (Fig. S1AB) while they were too cold by up to 1 °C south of 15°S, resulting in an overestimation of the meridional SST gradient and a root mean squared error (RMSE) of 0.62 °C. Temperatures at depth were generally colder than observations at 250 m (by up to 2 °C) and warmer at 600 m (by up to 1 °C) resulting in a mean RMSE of 1 °C (Fig. S1D). Finally, surface chlorophyll concentrations were underestimated (Fig. S1F) by 33% over most of the domain (RMSE of 0.052 $mg.m^3$). The NEMO-PISCES simulation systematically reduced these historical biases: the surface warm bias was weaker and more spatially homogeneous (RMSE of 0.5 °C), the bias at depth was reduced (RMSE of 0.62 °C) and the surface chlorophyll underestimation was reduced (by 20%, RMSE of 0.035 $mg.m^3$). These weaker biases for the present climate indicated that our forced NEMO-PISCES modelling strategy more adequately reproduced the ocean dynamical and biogeochemical structures in the Coral Sea than coupled ocean atmosphere CMIP5 models (this result not only applied to the IPSL model but also to the GFDL and MIROC models; not shown). Moreover, the season cycle in the Coral Sea of the SST and chlorophyll was closer to the observations in terms of absolute values for the NEMO-PISCES simulation than for the IPSL simulation (Fig. S1GH). The improved representation of the spatial structures and of the season cycle of chlorophyll and temperature with our bias mitigation strategy were expected to lead to more reliable future ocean states. Fig. S2 compared future projections for the IPSL and our NEMO-PISCES simulations and demonstrated that our bias-corrected strategy led indeed results in significant differences in terms of temperature and chlorophyll projections: our bias-corrected simulation projected a warming weaker than the one simulated by the IPSL model and an increased in surface chlorophyll north of 25°S, in a region where the IPSL model generally project a decrease.

From those, we computed one hindcast ocean climatology over the 1979–2009 period (CTL_{NM_CLIM}), and three forecast ocean climatologies over the 2070–2100 period calculated from the three climate change simulations ($GFDL_{NM\_CLIM}$, $MIROC_{NM\_CLIM}$ and $IPSL_{NM\_CLIM}$). Forecast relative changes were computed in % change relative to hindcast climatological values (e.g., $IPSL_{NM\_RC} = 100*(IPSL_{NM\_CLIM} - CTL_{NM\_CLIM}) / CTL_{NM\_CLIM}$).

Table 1
Ocean-Atmosphere coupled models and their related modelling centers used in this study (Taylor et al., 2012).

Modeling centers	Coupled models
Institut Pierre Simon Laplace (IPSL)	IPSL-CM5A-MR
Geophysical Fluid Dynamics Laboratory (NOAA GFDL)	GFDL-ESM2G
Japan Agency for Marine-Earth Science and Technology, Atmosphere and Ocean Research Institute (The University of Tokyo), and National Institute for Environmental Studies (MIROC)	MIROC-ESM

2.3. Micronekton models

2.3.1. The SEAPODYM model

The first micronekton model used was SEAPODYM, which has been widely used to predict Pacific tuna biomass and spatial distribution from the simulated micronekton in response to climate change and to support Pacific Island resource management (Johnson et al., 2018; Lehodey et al., 2010a,b, 2013, 2015a,b; Senina et al., 2016). The SEAPODYM-MTL (MTL: Mid Trophic Level) sub-model simulates several functional groups of micronekton for the oceanic epi-, upper meso- and lower meso-pelagic layers in the upper 1000 m (Lehodey et al., 2010a,b, 2015a,b). The spatial and temporal dynamics of production and biomass are modelled with a system of advection–diffusion-reaction equations driven by ocean temperature, horizontal currents and primary

production (Table 2). Currently, there are six groups of micronekton defined according to the DVM patterns of mesopelagic organisms between three broad epipelagic, upper and lower mesopelagic vertical layers: epipelagic, upper mesopelagic, lower mesopelagic, migrant upper mesopelagic, migrant lower mesopelagic and highly migrant lower mesopelagic. The euphotic depth Z_{eu} is used as a reference to the depth boundaries of the vertical layers, i.e., 0–1.5*Z_{eu} (about 0–150 m) for the epipelagic layer, 1.5–4.5*Z_{eu} (about 150–450 m) for the upper mesopelagic layer and 4.5–10.5*Z_{eu} (about 450–1000 m) for the lower mesopelagic layer. During the day, only the epipelagic group inhabits the epipelagic layer. During the night, this layer also hosts the migrant upper mesopelagic and highly migrant lower mesopelagic groups. The resident and migrant upper mesopelagic groups inhabit the upper mesopelagic layer during the day. During the night, this layer is inhabited by the resident upper mesopelagic and the migrant lower mesopelagic groups. Finally, the lower mesopelagic layer is inhabited by resident, migrant and highly migrant lower mesopelagic groups during the day but only the resident lower mesopelagic during the night (as the other groups have migrated upward, in the other layers, during the night).

The SEAPODYM-MTL model were forced by the four physical-biogeochemical outputs (CTL_{NM}, $GFDL_{NM}$, $MIROC_{NM}$ and $IPSL_{NM}$) detailed in Section 2.2, resulting in four SEAPODYM simulations: CTL_{SEA}, $IPSL_{SEA}$, $GFDL_{SEA}$, and $MIROC_{SEA}$ (Fig. 1C). From those, we computed one hindcast climatology (CTL_{SEA_CLIM}, over the 1979–2009 period), and three forecast climatologies ($IPSL_{SEA\_CLIM}$, $GFDL_{SEA\_CLIM}$, and $MIROC_{SEA\_CLIM}$, over the 2070–2100 period). Forecast relative changes were computed relative to hindcast climatological values (e.g., $IPSL_{SEA\_RC} = IPSL_{SEA\_CLIM}/CTL_{SEA\_CLIM} - 1$). A 1° horizontal resolution was employed.

2.3.2. Acoustic model

We compared SEAPODYM projections with those obtained by a 3-D statistical model developed by Receveur et al. (2019) which related micronekton vertical distribution obtained from acoustic data to environmental conditions in the Coral Sea region. Acoustic data collection, statistical methods and validation of micronekton biomass estimate in the New Caledonia EEZ were extensively detailed in Receveur et al. (2019). We briefly summarized its major components here.

Data were collected during six cruises in the study area 156°E–175°E and 14°S–27°S from 2011 to 2017, using an EK60 echo sounder (SIMRAD Kongsberg Maritime AS, Horten, Norway). After data processing, 38 kHz acoustic data was echo-integrated to provide the Nautical Area Scattering Coefficient (NASC, m^2nmi^{-2}), a proxy for the micronekton biomass (Irigoien et al., 2014; MacLennan, 2002; Proud et al., 2017). The final dataset gathered 16,715 acoustic vertical profiles ranging between 10 and 600 m depth, transition periods at dawn and dusk were excluded. A machine-learning model (Receveur et al., 2019) was used to robustly relate acoustic vertical profiles to the following explicit environmental variables: speed of the wind (measured by satellite), 0–600 m mean temperature and 0–600 m mean salinity (reprocessed data from at sea observation and satellite measurement), 0–600 m mean oxygen (reprocessed data from at sea observation), surface chlorophyll (measured by satellite), bathymetry (reprocessed from sonar data) and sun inclination. By integrating the predicted acoustic value (NASC) from the model over given depth ranges, we obtained a proxy of the micronekton biomass (i.e, the "acoustic" biomass) over the vertical layers.

We used here the same approach as Receveur et al. (2019) except that several environmental variables (mean temperature, mean oxygen, mean salinity, surface chlorophyll, winds) used to fit the acoustic data were extracted from the CTL_{NM_CLIM} dataset rather than from observations (see Table 2 and Receveur et al., 2019). In order to validate the use of CTL_{NM_CLIM} variables to predict realistic NASC values, the statistical model was fitted based on CTL_{NM_CLIM} variables and compared to that based on *in situ* variables.

Finally, the acoustic statistical model was used to predict NASC values from the four physical-biogeochemical outputs (CTL_{NM}, $GFDL_{NM}$, $MIROC_{NM}$ and $IPSL_{NM}$), resulting in four acoustic model simulations: CTL_{NASC}, $IPSL_{NASC}$, $GFDL_{NASC}$, and $MIROC_{NASC}$ (Fig. 1C). From those, we calculated the four climatologies over the same periods as SEAPODYM (CTL_{NASC_CLIM} over the 1979–2009 period; and $IPSL_{NASC\_CLIM}$, $GFDL_{NASC\_CLIM}$, and $MIROC_{NASC\_CLIM}$ over the 2070–2100 period). Forecast relative changes were computed relative to hindcast climatological values (e.g., $IPSL_{NASC\_RC} = IPSL_{NASC\_CLIM}/CTL_{NASC\_CLIM} - 1$).

2.3.3. Micronekton model inter-comparison

The NASC values were integrated vertically following the same vertical layers defined in SEAPODYM, i.e. proportionally to the euphotic depth (Section 2.2). The relative changes predicted from SEAPODYM and from the acoustic model were compared using Spearman correlation coefficient and for the three bias-mitigated forcing (i.e., $IPSL_{NASC\_RC}$ and $IPSL_{SEA\_RC}$; $GFDL_{NASC\_RC}$ and $GFDL_{SEA\_RC}$; and $MIROC_{NASC\_RC}$ and $MIROC_{SEA\_RC}$).

2.3.4. Micronekton biomass–physical projections comparison

Linear models were fitted to the SEAPODYM and acoustic model to test the influence of changes in each physical parameter on estimates of micronekton biomass. For each micronekton model and for the three bias-mitigated forcing, the relative biomass change (e.g., $IPSL_{NASC\_RC}$) was explained as a function of relative change of the six environmental variables (wind, mean temperature, mean oxygen, mean salinity, surface chlorophyll and currents extracted from $IPSL_{NM\_RC}$ for example). Variables were ranked in importance based on the absolute value of the t-statistic for each linear model parameter (Kuhn et al., 2020).

3. Results

3.1. Validation of the micronekton acoustic model using NEMO-PISCES variables

NASC values predicted with the acoustic model displayed similar spatial pattern when using *in situ* oceanographic data or CTL_{NM_CLIM} simulation outputs, with larger values south of 22°S (near New Caledonia) and smaller values to the north (Fig. 2A). Predictions based on *in situ* data were, however, higher than those derived from CTL_{NM_CLIM} data in the southern region. NASC values predicted from observed data

Table 2
Covariates used as forcing for the SEAPODYM and for the acoustic models. The last column gives the *in situ* sources used to validate the acoustic modeling. For salinity, 1 PSU is approximately equal to 1 g/kg; "-" indicate that the covariate was not used in the model.

Variable	Unit	SEAPODYM	Acoustic model	Sources to validate the acoustic modeling	References
Currents	m/s	Mean by vertical layer	–	–	–
Norm of winds	m/s	–	Surface	Cross-Calibrated Multi-Platform (CCMP-v2)	Wentz et al., 2015
Temperature	°C	Mean by vertical layer	0–600 m mean	ARMOR3D	Guinehut et al., 2012
Oxygen	$mmol/m^3$	Mean by vertical layer	0–600 m mean	CARS2009	Ridgway et al., 2002
Salinity	PSU (Practical Salinity Unit)	–	0–600 m mean	ARMOR3D	Guinehut et al., 2012
Chlorophyll	mg/m^3	Surface	Surface	GlobColour (MODIS/VIIRSN)	Saulquin et al., 2009
Bathymetry	km	–	Yes	ETOPO1	Amante and Eakins, 2009
Sun inclination	°	Yes	Yes	Calculated from position and date	Blanc and Wald, 2012

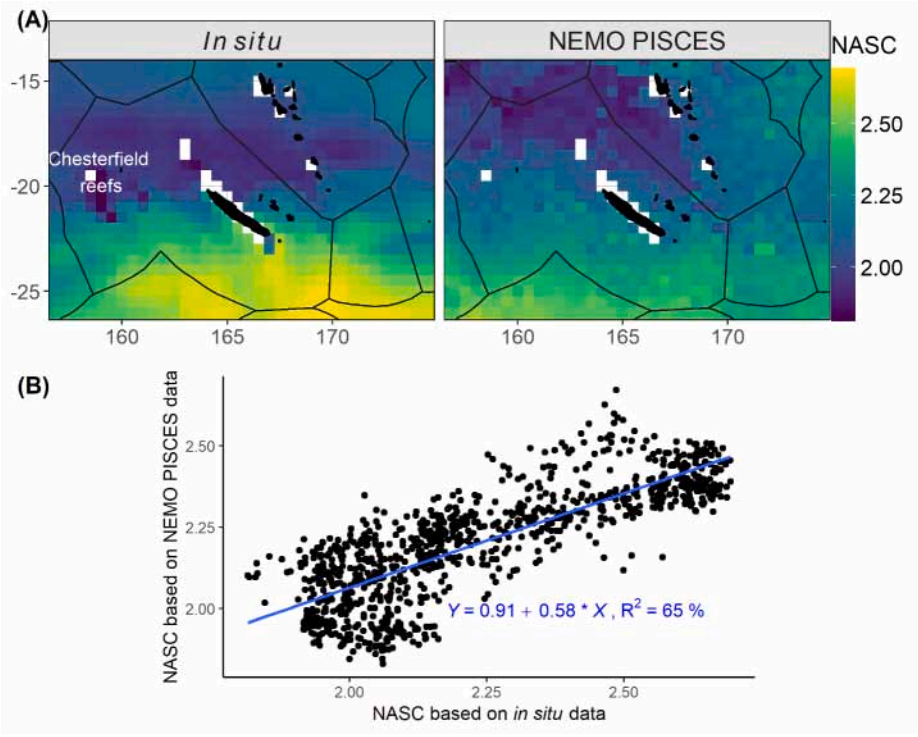

Fig. 2. Micronekton NASC (m^2nmi^{-2}) acoustic spatial predictions (2000–2010) based on *in situ* oceanographic data (A, left) and on NEMO-PISCES oceanographic data (A, right), and scatter plot of pooled values with NASC predicted based on *in situ* oceanographic data (*x-axis*) and on NEMO-PISCES oceanographic data (*y-axis*) (B).

display a minimum located near 18°S, while this minimum was further north ca. 16°S with CTL_{NM_CLIM} simulation. Some discrepancies were also evidenced at smaller scale, with, for instance, a local minimum around the Chesterfield reefs when using *in situ* oceanographic data but not present when using CTL_{NM_CLIM} simulation (because of the relatively coarse resolution of the model that does not adequately represent the associated bathymetry). Despite these biases, there was good agreement between NASC values predicted from *in situ* and CTL_{NM_CLIM} simulation, with a significant correlation coefficient of 0.81 (Fig. 2B). The slope coefficient was weaker than 1 (0.58), reflecting the overall underestimation of NASC when using NEMO-PISCES instead of *in situ* data (mostly stemming from the southern domain underestimations). Despite the bias to a lower range of values and the local discrepancies described above, results from the acoustic model with CTL_{NM_CLIM} variables was sufficiently accurate to assess the evolution of NASC using climate change projections

3.2. Hindcast situation of predicted micronekton biomasses

Hindcast patterns of micronekton biomasses within the epipelagic layer (Fig. 3, top panels) were similar for the NASC (CTL_{NASC_CLIM}) and SEAPODYM (CTL_{SEA_CLIM}) models, with a larger abundance south of 25°S compared to the northern part of the domain. While the acoustic model simulated a maximum at the southwestern boundary of the domain (i.e. in the Australian EEZ), the SEAPODYM model simulated a maximum at the southeastern boundary (i.e. close to the New Zealand EEZ). The correlation coefficient for the epipelagic biomasses between the two models was 0.79 ($R^2 = 0.63$).

In contrast, the vertical pattern simulated by the two models differed considerably for the two mesopelagic layers (Fig. 3, middle and bottom panels). Both model simulations exhibited large values south of 25°S latitude in the two mesopelagic layers but the biomass spatial distribution greatly differed in the northern part of the domain. The acoustic model simulated a hotspot north of the Fijian EEZ, which was absent in the SEAPODYM outputs. These mismatches resulted in insignificant spatial correlations between NASC and SEAPODYM values for both the upper meso-pelagic ($R^2 = 0.062$) and lower mesopelagic ($R^2 = 0.064$) layers.

3.3. Micronekton projected changes

3.3.1. Biomass pattern changes

3.3.1.1. Epipelagic layer. Fig. 4 displayed the biomass response to climate change in the epipelagic layer simulated by the two micronekton models for the three bias-mitigated forcing used. There was general agreement between the two models for projected changes, with the pattern correlations (e.g., pattern correlation for the pooled relative change values on Fig. 4 'GFDL-SEAPO' and 'GFDL-NASC' panels) between each of the two models and the three bias-mitigated forcing being significant and positive (Table 3). Both micronekton models both indicated a forecast biomass decrease in the southern part of the Coral Sea, south of the latitude 21°S, for the three bias-mitigated forcing. The amplitude of the projected decrease in the southern part was however smaller for the acoustic model (e.g., ~−5% on average south of 20°S in $IPSL_{NASC\_RC}$) compared to the SEAPODYM model (~−20% on average south of 20°S in $IPSL_{SEAPO\_RC}$). The northern part of the domain generally experienced a biomass increase but this prediction was less consistent among the three bias-mitigated forcing. The two micronekton models predict a maximum increase in the Fijian economic zone when based on $IPSL_{NM}$ and $GDFL_{NM}$. Projected patterns and amplitude based on $MIROC_{NM}$ however differed in the northern part compared to those on $IPSL_{NM}$ and $GDFL_{NM}$ for each micronekton model. For the acoustic model, MIROC forcing only induced a small increase (~+1% on average in $IPSL_{NASC\_RC}$) in a very narrow latitudinal band located in the central part of the Coral Sea [20°S, 17°S] and a further decrease north of 17°S (~−6% on average in $IPSL_{NASC\_RC}$). These changes differed compared to the other acoustic projections (~+14% in $IPSL_{NASC\_RC}$ and ~+12% in

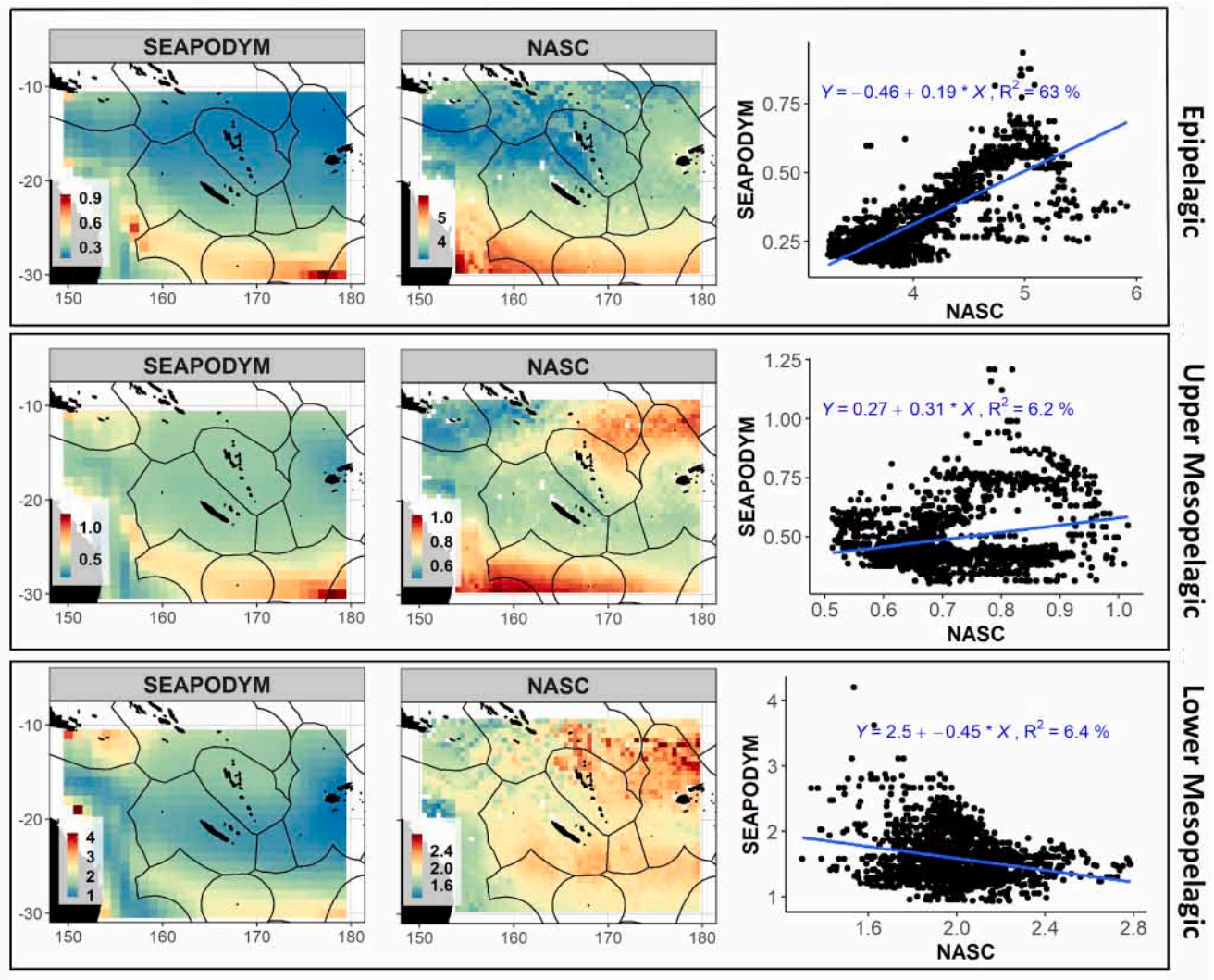

Fig. 3. Hindcast (1979–2009) micronekton biomass simulated by (left column) the SEAPODYM model (in g/m^2) and (second column) the acoustic model (m^{2}nmi^{-2}) and (right column) relationship between the biomass in the two models over (top) the epipelagic zone (about 0–150 m), (middle) the upper mesopelagic zone (about 150–450 m), and (bottom) the lower mesopelagic zone (about 450–1000 m). The blue line on right panels indicate the linear regression slope. EEZ used in the manuscript (black outlines) are indicated on the first map (PNG: Papua New Guinea; SB: Solomon island; AU: Australia; NC: New Caledonia, VU: Vanuatu; FJ: Fiji; NF: Norfolk islands; NZ: New Zealand). (For interpretation of the references to color in this figure legend, the reader is referred to the web version of this article.)

IPSL$_{NASC_RC}$ on average north of 20°S). For the SEAPODYM model, the MIROC forcing induced a larger increase (~+20% on average north of 20°S) that was shifted to the west in the northern part compared to the IPSL and GFDL forcing (respectively ~+3.2% and ~+4% on average north of 20°S).

Overall, both micronekton models generally predicted a very consistent decrease of the epipelagic biomass in the southern Coral Sea and a more variable increase to the north (Fig. 4), resulting in a future decrease of the meridional gradient of micronekton biomass characterizing hindcast conditions (Figs. S3 and S4).

3.3.1.2. Upper mesopelagic layer. Patterns of biomass changes in the upper mesopelagic layer projected by the SEAPODYM model (Fig. 5, bottom panels) resembled those for the epipelagic layer (Fig. 4, bottom panels), with a decrease in the southern part of the domain (~−15% on average south of 20°S and for the three bias-mitigated forcing) and an increase in the north (~+8% on average north of 20°S and for the three bias-mitigated forcing). Patterns slightly varied depending on the bias-mitigated forcing considered, with a maximum increase around the Solomon Islands for MIROC$_{SEA_RC}$ and near Vanuatu and Fiji for GFDL$_{SEA_RC}$ and IPSL$_{SEA_RC}$.

Patterns projected by the acoustic model were less consistent between the different bias-mitigated forcing. The decrease in the south identified in all the SEAPODYM projections only occurred using IPSL$_{NASC_RC}$ in the acoustic model. Similarly, GFDL$_{NASC_RC}$ and IPSL$_{NASC_RC}$ showed a biomass increase north of the latitude 13°S, while the signal was opposite in MIROC$_{NASC_RC}$. As a result, predicted acoustic patterns were not well correlated to SEAPODYM patterns in the upper mesopelagic layer compared to the epipelagic layer (Table 3).

3.3.1.3. Lower mesopelagic layer. Lower mesopelagic layers projected in the SEAPODYM model (Fig. 6, bottom panels) displayed a meridional dipolar structure similar to those of the epipelagic and upper mesopelagic layer (Figs. 4 and 5, bottom panels) for the three bias-mitigated forcing. The relative northern biomass increase was however more pronounced (~+15% on average north of 20°S and for the three bias-mitigated forcing) for that layer compared to the epipelagic and upper mesopelagic layers (respectively ~+2% and ~+6% on average north of 20°S and for the three bias-mitigated forcing).

In contrast, projected patterns with the acoustic model in the lower mesopelagic layer (Fig. 6, top panel) differed from the patterns in two other layers (Figs. 4 and 5, botom panels) and for the different bias-

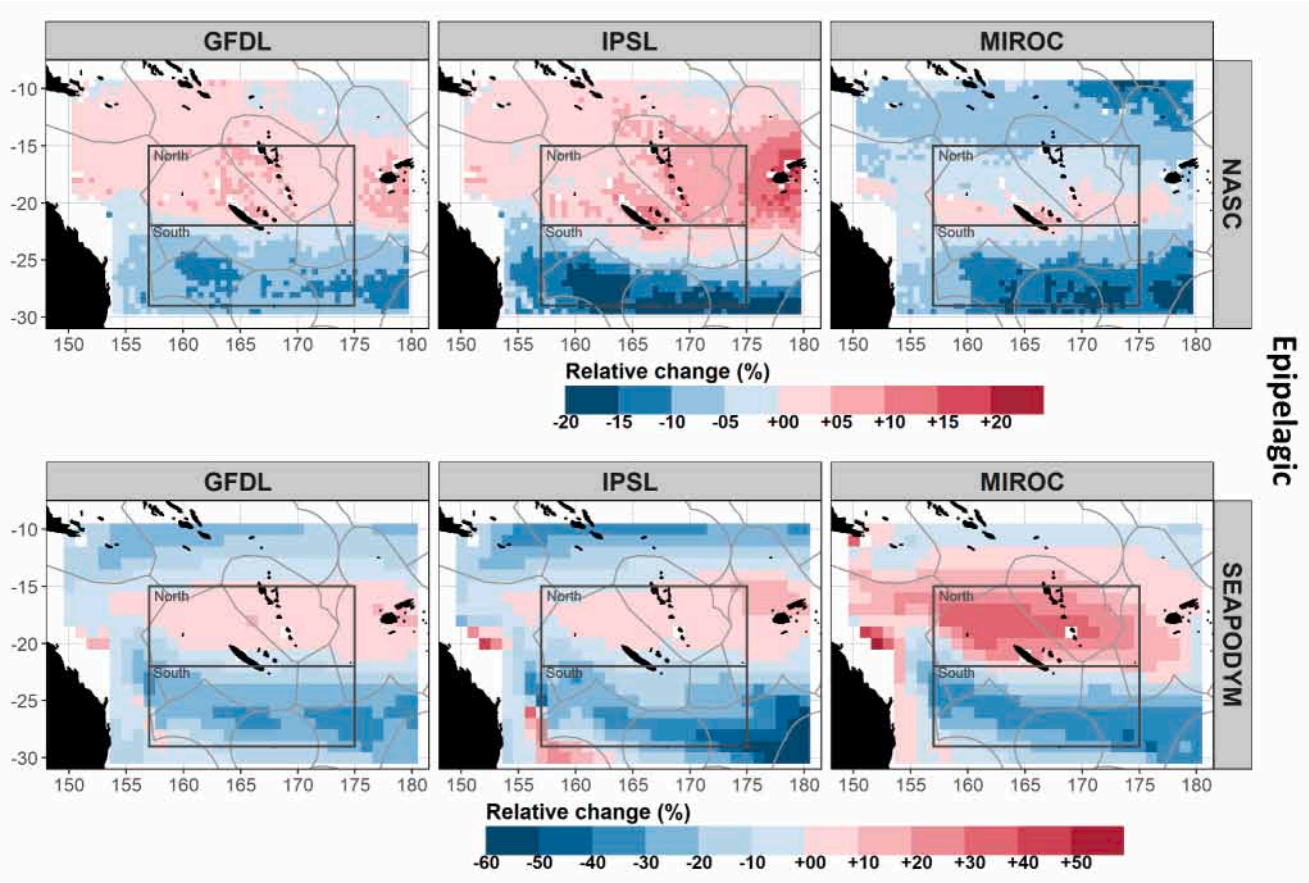

Fig. 4. Relative change (in %) of micronekton biomass in the epipelagic zone (about 0–150 m) between 2070 and 2100 and 1979–2009 projected for (top) the acoustic model and (bottom) SEAPODYM forced with three bias-mitigated physical and biogeochemical models (GFDL, IPSL and MIROC; see Table 1 for explanations of the acronym; see Section 2 for details). Grey box shows the region used to produce Fig. 7. Note that color scales are different for the NASC and SEAPODYM predictions.

Table 3
Spearman pattern correlations between SEAPODYM relative change and NASC relative change for the three atmospheric forcing and by vertical layer. (*) indicates significant results for a 0.01 threshold.

	Epipelagic	Upper mesopelagic	Lower mesopelagic
GFDL	0.73 (*)	−0.31 (*)	−0.12
IPSL	0.54 (*)	0.34 (*)	−0.16
MIROC	0.71 (*)	−0.45 (*)	−0.7 (*)

mitigated forcing used. While $GFDL_{NM}$ and $IPSL_{NM}$ forcing induced a biomass increase almost everywhere (~+8% on average for all $GFDL_{NASC\_RC}$ and $IPSL_{NASC\_RC}$ values) with similar patterns, $MIROC_{NM}$ forcing induced a strong biomass decrease north of 20°S (~−13% on average in $MIROC_{NASC\_RC}$ north of 20°S). The correlations between projected patterns between the acoustic model and SEAPODYM were insignificant (Table 3).

3.3.2. Total biomass changes

Fig. 7 displayed the inter-model (GFDL, IPSL and MIROC) mean changes in micronekton biomass for each layer and averaged over two homogenous spatial boxes. Both acoustic and SEAPODYM models projected a biomass decrease in the southern box for the epipelagic layer (−10.2% and −29.4% respectively) and for the upper mesopelagic layer (−2% and −24.3% respectively). In contrast, the biomass was projected to slightly increase in the northern box for the epipelagic layer for both micronekton models (+2.4% and + 8.3% respectively). Relative changes were less consistent for the lower mesopelagic layer with a large increase in the north and a large decrease in the south (respectively + 23% and −17.9%) predicted by SEAPODM while acoustic projections showed little change in the north and an increase in the south (+6.8%). All temporal trends were significant except in the lower mesopelagic layer for NASC values.

The interannual variability between 1979 and 2100 was important for both the acoustic and SEAPODYM models and for all layers (Fig. 7). In SEAPODYM simulations, interannual biomass variations were larger for the epipelagic layer compared to the lower mesopelagic layer, whereas acoustics simulations displayed larger interannual variability in lower mesopelagic projections.

3.3.3. Drivers of the biomass changes

The environmental response to climate change simulated by NEMO-PISCES over the Coral Sea was generally consistent for the three different bias-mitigated forcing, with the exception of salinity (Fig. S5). Results from multi-linear regressions indicated that projected changes in chlorophyll and temperature exerted a strong control on the future evolution of epipelagic biomass in the Coral Sea (Table 4). Conversely, salinity and current had the lowest influence among parameters tested, both for SEAPODYM and NASC projections. When comparing the influence of environmental variables across bias-mitigated forcing, there was, a general consistency concerning the most influential parameters.

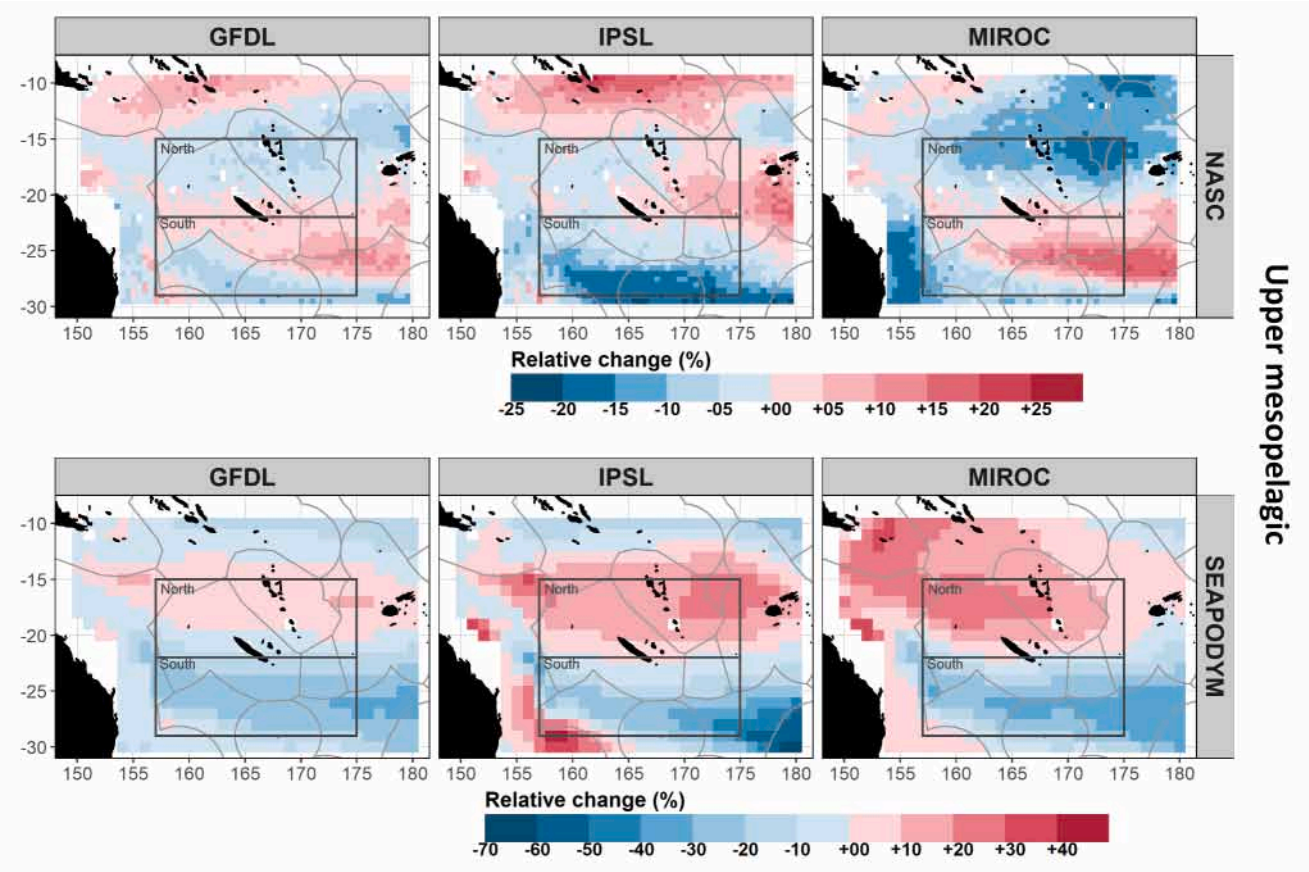

Fig. 5. Same as Fig. 4 but for the upper-mesopelagic zone (about 150–450 m).

4. Discussion

4.1. Summary of the results

The present study provided the first assessment of the future changes expected for mid-trophic level organisms in the Coral Sea, a well-known biodiversity hot spot (Payri et al., 2019; Ceccarelli et al., 2013). Two micronekton models forced by three different bias-mitigated forcing datasets predicted relatively consistent patterns of biomass change in the epipelagic layer (~0–150 m) by 2100, with a marked decrease south of 22°S and a weaker increase further north. In contrast, spatial patterns of biomass change differed considerably between the two micronekton models in the two mesopelagic layers. The SEAPODYM model generally predicted a meridional dipolar pattern in both mesopelagic layers similar to the one predicted for the epipelagic layer, and was relatively consistent across the three bias-mitigated forcing. In contrast, the acoustic model projected different patterns in mesopelagic layers compared to the epipelagic layer with less consistent patterns between the different bias-mitigated forcing.

4.2. Considerations on the physical modelling strategy

The two micronekton models were forced by the NEMO-PISCES simulations based on a bias mitigated strategy. For the hindcast period, this strategy allowed to simulate more reliable conditions compared to the uncorrected CMIP5 simulations (Fig. S1). The strategy modified the forecast conditions too (Fig. S2). For instance, the chlorophyll spatial pattern changes differed between our NEMO-PISCES simulation and the CMIP5 IPSL simulation: a north–south dipole appeared in our simulation that was weaker and more pronounced to the north in the CMIP5 IPSL simulation.

Noteworthy, our bias-mitigated strategy assumed that CMIP5 biases were stationary over time, i.e. that model projections were independent from their present-day biases. However, recent publications question this assumption. For instance, Li et al. (2016) showed that the cold tongue bias in the equatorial Pacific simulated by most CMIP models induces an overestimation of the projected warming in the western Pacific, hence pointing to an influence of present-day SST biases on CMIP5 models in this region. This work should be seen as a first attempt to simulate the trends of the micronekton biomasses in the WSTP. Further developments are however needed to refine the bias correction strategy used by reducing further present-day NEMO-PISCES biases in our region of interest but also by correcting future CMIP5 forcing using bias mitigation technics such as emergent constraint method in the region (e.g. Dutheil et al., 2019; Brown et al. 2020).

4.3. Comparison with previous studies

Several studies focusing on future changes of marine animals have projected a decline of marine biomass in the tropical regions (Cheung et al., 2016b; Kwiatkowski et al., 2019; Lotze et al., 2019). Bryndum-Buchholz et al. (2019) noted a micronekton biomass decrease reaching ~ −15% for 0–30 cm length organisms for the whole South Pacific Ocean, and Lefort et al. (2015) noted a ~ −20% decrease for the whole Pacific Ocean. However, how the ecological changes may play out at regional scale had not been comprehensively explored and understood. Our predictions were consistent with Bryndum-Buchholz et al. (2019) and Lefort et al. (2015), as we found a mean decrease of the micronekton biomass over the whole Coral Sea (~−10% for combined outputs of both models). However, our study provided additional insights on these projected changes, demonstrating heterogeneous changes vertically and horizontally with an important regional spatial variability. Within the

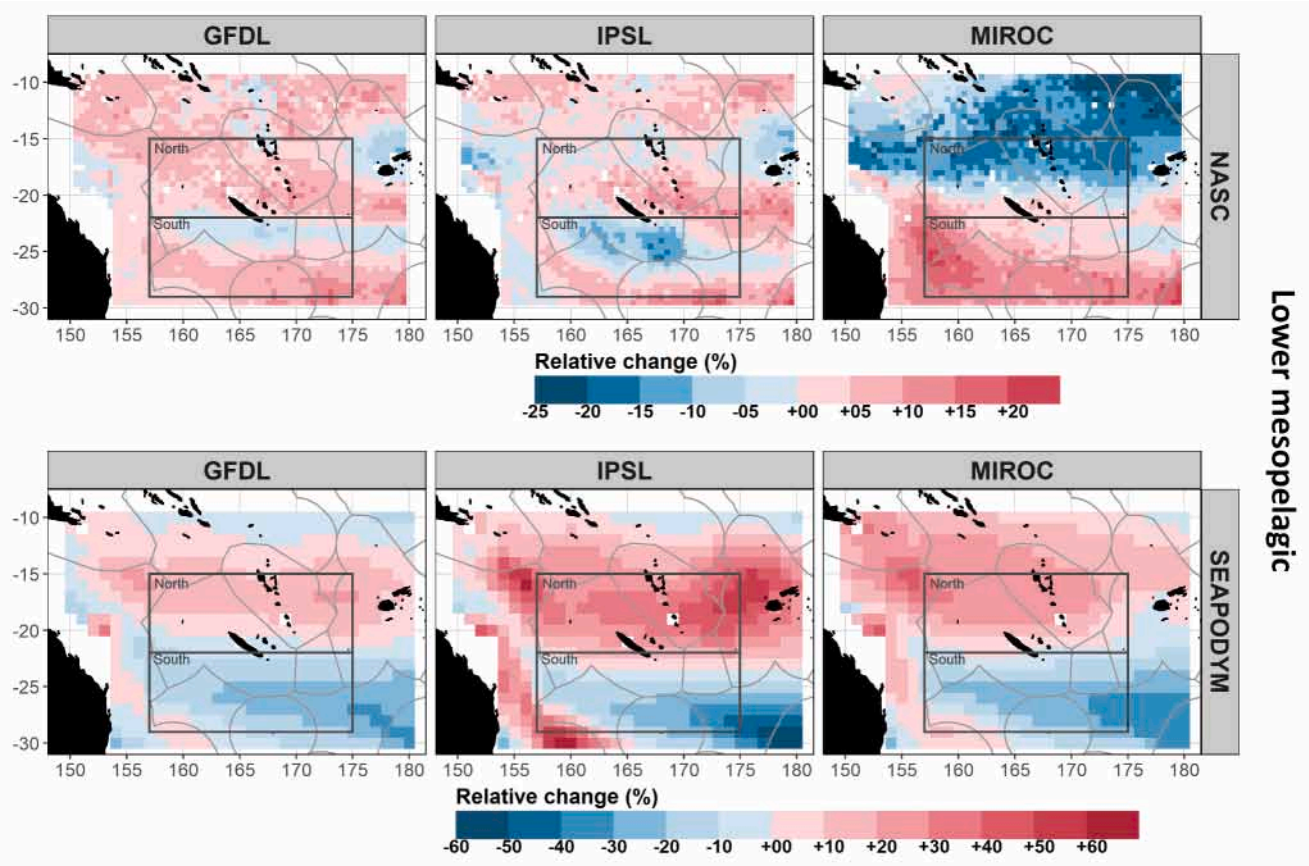

Fig. 6. Same as Figs. 4 and 5 but for the lower-mesopelagic zone (about 450–1000 m).

Coral Sea, both micronekton models predicted a dipole pattern of the projected changes in the epipelagic layer, across the three bias-mitigated forcing, with an increase of micronekton abundance in the north (about + 2.4% and + 8% for the acoustic and SEAPODYM models respectively) and a decrease south of 22°S (about −10% and −30% for the acoustic and SEAPODYM models respectively). These contrasted spatial changes were consistent with the global map of changes shown by Lefort et al. (2015). The differences in projections among the three vertical layers based on the acoustic model showed that the integration of a 3-dimensional structure is needed for a complete and robust understanding of the future change of micronekton biomass.

Our marine biomass projections were sensitive to the micronekton model used and also the climate forcing, especially in the mesopelagic layers. Many sources of uncertainty exist when marine biomasses are projected in the future: the structure of the model (e.g., age-structured, length-structured, individual based model); the methodology to estimate model parameters (e.g., based or not on comparison to observed values); the type of forcing applied; and the scenario used to produce the forcing. Among these, several studies pointed out that the largest uncertainties were mostly linked to the scenario considered, especially for the marine ecosystems (Bonan and Doney, 2018; Cheung et al., 2016a; Payne et al., 2016). In the present study, we presented bias mitigated forcing for only one scenario, RCP8.5, the highest emissions scenario. Therefore, using additional scenarios and especially the ones including greenhouse gas mitigation policies (e.g., SSP2) would further help quantify the uncertainty of future projections. Also, while regional downscaling of climate model outputs will become available, it will be essential to investigate the sensitivity of these results using higher spatial resolution.

4.4. Main drivers of the biomass changes

Chlorophyll changes displayed a dipolar structure located at ~ 22°S, qualitatively matching the seasonal boundary between the oligotrophic waters of the Coral Sea and the more productive waters found in the Tasman Seas (Menkes et al., 2015). Biogeochemical model outputs indicated that oligotrophic waters to the north were expected to become more productive while chlorophyll-rich waters to the south should become less productive, hence reducing the meridional chlorophyll gradient in the Coral Sea region (Fig. S5). In NEMO-PISCES future simulations, density (thermal) stratification tended to increase under global warming as expected which resulted in increased nutrient stratification thus reducing the amount of nutrient fluxes in the surface layer and in turns reducing primary production. The chlorophyll-change patterns were consistent with the epipelagic biomass decrease in the south and increase in the north. This positive relationship between primary production and mesopelagic organisms has been well documented for present-day oceanic conditions (Boersch-Supan et al., 2017; Escobar-Flores et al., 2013; Irigoien et al., 2014; Receveur et al., 2020a).

Our results pointed towards an increase (or relatively smaller decrease) in epipelagic micronekton biomass in waters experiencing enhanced warming using both SEAPODYM and acoustic models (Fig. S5). Aside its direct influence on micronekton, the temperature influences the primary production following two counteracting mechanisms: (1) an enhanced warming leads to faster metabolic processes and therefore higher primary production; and (2) enhanced surface warming also leads to increased upper ocean stability, reducing the efficiency of vertical mixing to bring more nutrients to the photic layer, and may therefore reduces primary production. A combination of these two counteracting processes certainly occurs in the Coral Sea. At the regional level, the statistical correlation between temperature, and secondary and tertiary biomasses become less clear due to the increasing influence

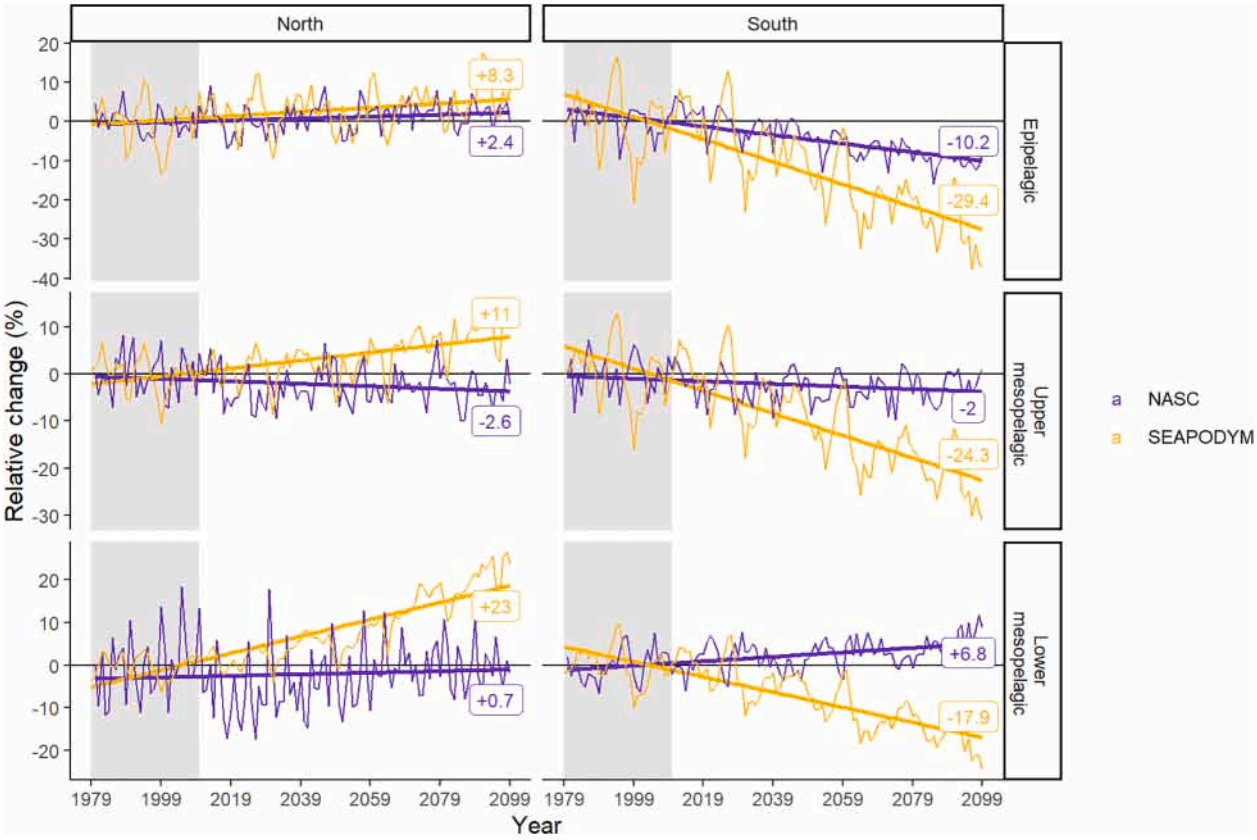

Fig. 7. Mean relative change of micronekton biomass (vertical axis) are presented for the acoustic model (purple) and SEAPODYM (yellow), relative to 1979–2009 (period identified by the grey square) for each vertical layer (rows) and for the two spatial regions (columns, see previous Figures) and on average over the three bias-mitigated forcing. Thick colored lines show a linear trend fitted and colored number give the mean change for the last 30 years. The black horizontal lines identify the zero. All temporal trend were significant except in the lower mesopelagic layer for NASC values. (For interpretation of the references to color in this figure legend, the reader is referred to the web version of this article.)

Table 4
Ranks of influence of physical and biogeochemical variables in linear statistical models to predict epipelagic values based on acoustics modeling and SEAPODM (rows) and for the three climate forcing (columns). Variables are ranked based on the absolute value of the *t*-statistic for each linear model parameter (Kuhn et al., 2020). The last two columns give the mean rank across the three climate forcing and the final importance rank per physical and biogeochemical variables.

ACOUSTIC	GFDL	IPSL	MIROC	Mean	Final rank
Chlorophyll	1	2	1	1.3	**1**
Wind	5	1	6	4.0	**4**
Salinity	4	6	4	4.7	**5**
Oxygen	3	3	5	3.7	**3**
Temperature	2	4	2	2.,7	**2**
Current	6	5	3	4.7	**6**
SEAPODYM	**GFDL**	**IPSL**	**MIROC**	**Mean**	**Final rank**
Chlorophyll	1	4	1	2.0	**1 ex-aequo**
Wind	6	2	5	4.3	**4**
Salinity	4	6	4	4.7	**5**
Oxygen	3	3	2	2.7	**3**
Temperature	2	1	3	2.0	**1 ex-aequo**
Current	5	5	6	5.3	**6**

of other mechanisms operating at this scale. These mechanisms include transport by currents, water mass dynamics, mesoscale aggregation and topographic effects. The effect of temperature discussed in the present study certainly encompasses more complex interactions with notably changes in vertical stratification that leads to changes in micronekton.

In SEAPODYM, with the change in primary production propagating to zooplankton and micronekton, the projected warming leads to faster turnover of organisms. A higher temperature generates a higher rate of natural mortality and earlier recruitment age (then, production) in the functional group. As a result, for a same amount of primary production, a warmer environment leads to lower biomass but higher production of micronekton. The relationship between the acoustic values and temperature is more complicated. It is the shape of a complete vertical profile that is linked to the environmental parameters, and moreover the link was estimated based on a Machine learning model that does not have a simple fitted relationship (Receveur et al., 2019).

The present study is a first step to estimate how changes in micronekton may affect higher trophic levels. However, to achieve this goal, it is also essential to understand how the transfer efficiencies from (1) gross and net production to (2) micronekton and (3) higher trophic level organisms will change in the future. These energy efficiency changes are indeed as important, if not more, than absolute changes in biomass (Delpech et al., 2020).

4.5. *Improve prediction reliability*

Our results revealed large differences in the micronekton biomass changes projected by SEAPODYM and the acoustic model for the mesopelagic layers, highlighting the need to improve our understanding and modeling of this deeper biological component.

Micronekton is composed of many species but both SEAPODYM and the acoustic model simulate a generic micronekton biomass without considering species specificities. However, each micronekton species has a specific habitat (Duffy et al., 2017; Receveur et al., 2020b). If a habitat becomes unsuitable for a given species, its abundance may decline by negatively affecting eco-physiological performances (e.g.

metabolic rates or growth) (Hillebrand et al., 2018; Pörtner, 2001) or it distribution may shift to cooler waters (Pecl et al., 2017). New environmental conditions may be also physiologically tolerable via acclimatization (an adjustment of physiology like oxygen tolerance by individual) or adaptation (increased abundance and reproduction with some genotype changes over generations) (Parmesan, 2006). Our models do not account for such biological plasticity since acoustic and SEAPODYM models were constructed respectively from statistically and deterministic relationships derived from a total micronektonic biomass. So far, given the micronekton species diversity already observed (Receveur et al., 2020b; Payri et al., 2019), the understanding of climate change effect on individual species cannot be envisioned in the near future in the Coral Sea. Moreover, the acoustic response of species communities may differ between regions or seasons characterized by different temperature regimes. In the future, it will be crucial to understand the fundamental differences in the way temperature affects each of the two micronekton models.

Further investigations are needed to understand why SEAPODYM and acoustic projections agreed well for the epipelagic layer but not for the mesopelagic layers. As the acoustic model uses complete acoustic vertical profiles (0–600 m) as an unit to explore, its predictions are expected to be equally reliable through the entire water column. However, the acoustic signal that is modelled may be not coherent enough over the full spatial domain and all seasons if sampled species communities are too different. About SEAPODYM, the model is layer-dependent and is sensitive to the way DVM is parameterized. Reliable predictions in one vertical layer does not ensure reliable predictions in the others.

In order to be able to fully explain the discrepancies in mesopelagic layers, a better understanding is required for transforming acoustic estimates into biomass. This would theoretically require the knowledge of the species composition of the micronekton community and how individual targets respond acoustically, a significant challenge given existing knowledge of community composition in the Coral Sea. Ideally a program of *in situ* sampling with appropriate trawls to identify the species composition of the different layers would resolve this uncertainty and lead to improved model reliability. This would allow (1) to link species to their environmental tolerances, (2) to characterize the micronekton communities by vertical layers and finally (3) to potentially assess biomass from acoustic signal for a better comparison with the biomass units used in SEAPODYM. It is also possible to reverse the comparison, i.e., transform the SEAPODYM outputs into acoustic values and make the comparison in the space of acoustic. This second option would require less specific knowledge on each species acoustic answer and appeared more feasible (Handegard et al., 2013).

4.6. Concluding remarks

We used an innovative bias-mitigated framework of atmospheric, oceanographic, and biogeochemical modelled variables to predict a decrease of micronekton biomass in the Coral Sea by 2100 for two micronekton models forced by 3 CMIP5 outputs under the RCP8.5 scenario. While micronekton biomass projections were consistent between both micronekton models and the three physical-biogeochemical model forcing used for the epipelagic layer, this was not the case for the two mesopelagic layers. Those inconsistencies emphasized the need to better observe and understand the micronekton species compositions and their acoustic responses to more robustly model their biomass distributions and to provide a more reliable assessment of the future ocean. Finally, our results also emphasized the need to better understand the mechanisms and processes (i.e., influence of physical and biogeochemical parameters on the different trophic level and the energy transfer across the trophic levels) that lead to biomass changes.

Declaration of Competing Interest

The authors declare that they have no known competing financial interests or personal relationships that could have appeared to influence the work reported in this paper.

Acknowledgements

This document has been produced with the financial assistance of the European Union. The contents of this document are the sole responsibility of A. Receveur and can under no circumstance be regarded as reflecting the position of European Union. We thank R/V ALIS officers and crews and science parties who participated to the cruises which data are included in the present paper. This work was supported by the French national program LEFE/INSU.

Appendix A. Supplementary material

Supplementary data to this article can be found online at https://doi.org/10.1016/j.pocean.2021.102593.

References

Allain, V., Fernandez, E., Hoyle, S.D., Caillot, S., Jurado-Molina, J., Andréfouët, S., Nicol, S.J., 2012. Interaction between Coastal and Oceanic Ecosystems of the Western and Central Pacific Ocean through Predator-Prey Relationship Studies. PLOS ONE 7, e36701. https://doi.org/10.1371/journal.pone.0036701.

Amante, C., Eakins, B.W., 2009. ETOPO1 1 ARC-MINUTE GLOBAL RELIEF MODEL: PROCEDURES, DATA SOURCES AND ANALYSIS (NOAA Technical Memorandum No. 24), NESDIS NGDC. National Geophysical Data Center Marine Geology and Geophysics Division, Boulder, Colorado.

Anderson, T.R., Martin, A.P., Lampitt, R.S., Trueman, C.N., Henson, S.A., Mayor, D.J., 2019. Quantifying carbon fluxes from primary production to mesopelagic fish using a simple food web model. ICES J. Mar. Sci. 76, 690–701. https://doi.org/10.1093/icesjms/fsx234.

Ariza, A., Garijo, J.C., Landeira, J.M., Bordes, F., Hernández-León, S., 2015. Migrant biomass and respiratory carbon flux by zooplankton and micronekton in the subtropical northeast Atlantic Ocean (Canary Islands). Prog. Oceanogr. 134, 330–342. https://doi.org/10.1016/j.pocean.2015.03.003.

Aumont, O., Ethé, C., Tagliabue, A., Bopp, L., Gehlen, M., 2015. PISCES-v2: an ocean biogeochemical model for carbon and ecosystem studies. Geosci. Model Dev. 8, 2465–2513. https://doi.org/10.5194/gmd-8-2465-2015.

Barange, M., Merino, G., Blanchard, J.L., Scholtens, J., Harle, J., Allison, E.H., Allen, J.I., Holt, J., Jennings, S., 2014. Impacts of climate change on marine ecosystem production in societies dependent on fisheries. Nat. Clim. Change 4, 211–216. https://doi.org/10.1038/nclimate2119.

Bell, J.D., Ganachaud, A., Gehrke, P.C., Griffiths, S.P., Hobday, A.J., Hoegh-Guldberg, O., Johnson, J.E., Le Borgne, R., Lehodey, P., Lough, J.M., Matear, R.J., Pickering, T.D., Pratchett, M.S., Gupta, A.S., Senina, I., Waycott, M., 2013. Mixed responses of tropical Pacific fisheries and aquaculture to climate change. Nat. Clim. Change 3, 591–599. https://doi.org/10.1038/nclimate1838.

Bertrand, A., Bard, F.-X., Josse, E., 2002. Tuna food habits related to the micronekton distribution in French Polynesia. Mar. Biol. 140, 1023–1037. https://doi.org/10.1007/s00227-001-0776-3.

Bianchi, D., Mislan, K.A.S., 2016. Global patterns of diel vertical migration times and velocities from acoustic data: Global patterns of diel vertical migration. Limnol. Oceanogr. 61, 353–364. https://doi.org/10.1002/lno.10219.

Bianchi, D., Stock, C., Galbraith, E.D., Sarmiento, J.L., 2013. Diel vertical migration: Ecological controls and impacts on the biological pump in a one-dimensional ocean model. Glob. Biogeochem. Cycles 27, 478–491. https://doi.org/10.1002/gbc.20031.

Blanc, P., Wald, L., 2012. The SG2 algorithm for a fast and accurate computation of the position of the Sun for multi-decadal time period. Sol. Energy 86, 3072–3083. https://doi.org/10.1016/j.solener.2012.07.018.

Blanchard, J., Jennings, S., Holmes, R., Harle, J., Merino, G., Allen, J.I., Holt, J., Dulvy, N.K., Barange, M., 2012. Potential consequences of climate change for primary production and fish production in large marine ecosystems. Philos. Trans. R. Soc. B Biol. Sci. 367, 2979–2989. https://doi.org/10.1098/rstb.2012.0231.

Boersch-Supan, P.H., Rogers, A.D., Brierley, A.S., 2017. The distribution of pelagic sound scattering layers across the southwest Indian Ocean. Deep Sea Res. Part II Top. Stud. Oceanogr. Pelagic Ecol. Seamounts South West Indian Ocean 136, 108–121. https://doi.org/10.1016/j.dsr2.2015.06.023.

Bonan, G.B., Doney, S.C., 2018. Climate, ecosystems, and planetary futures: The challenge to predict life in Earth system models. Science 359. https://doi.org/10.1126/science.aam8328.

Bopp, L., Resplandy, L., Orr, J.C., Doney, S.C., Dunne, J.P., Gehlen, M., Halloran, P., Heinze, C., Ilyina, T., Séférian, R., Tjiputra, J., Vichi, M., 2013. Multiple stressors of ocean ecosystems in the 21st century: projections with CMIP5 models. Biogeosciences 10, 6225–6245. https://doi.org/10.5194/bg-10-6225-2013.

Boussarie, G., Bakker, J., Wangensteen, O.S., Mariani, S., Bonnin, L., Juhel, J.-B., Kiszka, J.J., Kulbicki, M., Manel, S., Robbins, W.D., Vigliola, L., Mouillot, D., 2018. Environmental DNA illuminates the dark diversity of sharks. Sci. Adv. 4, eaap9661. https://doi.org/10.1126/sciadv.aap9661.

Brown, J.R., Lengaigne, M., Lintner, B.R., Widlansky, M.J., van der Wiel, K., Dutheil, C., Linsley, B.K., Matthews, A.J., Renwick, J., 2020. South Pacific Convergence Zone dynamics, variability and impacts in a changing climate. Nat. Rev. Earth Environ. 1, 530–543. https://doi.org/10.1038/s43017-020-0078-2.

Bryndum-Buchholz, A., Tittensor, D.P., Blanchard, J.L., Cheung, W.W.L., Coll, M., Galbraith, E.D., Jennings, S., Maury, O., Lotze, H.K., 2019a. Twenty-first-century climate change impacts on marine animal biomass and ecosystem structure across ocean basins. Glob. Change Biol. 25, 459–472. https://doi.org/10.1111/gcb.14512.

Cai, W., Santoso, A., Wang, G., Yeh, S.-W., An, S.-I., Cobb, K.M., Collins, M., Guilyardi, E., Jin, F.-F., Kug, J.-S., Lengaigne, M., McPhaden, M.J., Takahashi, K., Timmermann, A., Vecchi, G., Watanabe, M., Wu, L., 2015. ENSO and greenhouse warming. Nat. Clim. Change 5, 849–859. https://doi.org/10.1038/nclimate2743.

Ceccarelli, Daniela M., McKinnon, A.D., Andrefouet, S., Allain, V., Young, J., Gledhill, D. C., Flynn, A., Bax, N.J., Beaman, R., Borsa, P., Brinkman, R., Bustamante, R.H., Campbell, R., Cappo, M., Cravatte, S., D'Agata, S., Dichmont, C.M., Dunstan, P.K., Dupouy, C., Edgar, G., Farman, R., Furnas, M., Garrigue, C., Hutton, T., Kulbicki, M., Letourneur, Y., Lindsay, D., Menkes, C., Mouillot, D., Parravicini, V., Payri, C., Pelletier, B., de Forges, B.R., Ridgway, K., Rodier, M., Samadi, S., Schoeman, D., Skewes, T., Swearer, S., Vigliola, L., Wantiez, L., Williams, Alan, Williams, Ashley, Richardson, A.J., 2013a. The Coral Sea: Physical Environment, Ecosystem Status and Biodiversity Assets, in: Lesser, M. (Ed.), Advances in Marine Biology, Vol 66. pp. 213-+. Doi: 10.1016/B978-0-12-408096-6.00004-3.

Cheung, W.W.L., Frölicher, T.L., Asch, R.G., Jones, M.C., Pinsky, M.L., Reygondeau, G., Rodgers, K.B., Rykaczewski, R.R., Sarmiento, J.L., Stock, C., Watson, J.R., 2016a. Building confidence in projections of the responses of living marine resources to climate change. ICES J. Mar. Sci. 73, 1283–1296. https://doi.org/10.1093/icesjms/fsv250.

Cheung, W.W.L., Lam, V.W.Y., Sarmiento, J.L., Kearney, K., Watson, R., Zeller, D., Pauly, D., 2010. Large-scale redistribution of maximum fisheries catch potential in the global ocean under climate change. Glob. Change Biol. 16, 24–35. https://doi.org/10.1111/j.1365-2486.2009.01995.x.

Cheung, W.W.L., Reygondeau, G., Frölicher, T.L., 2016b. Large benefits to marine fisheries of meeting the 1.5°C global warming target. Science 354, 1591–1594. https://doi.org/10.1126/science.aag2331.

Delpech, A., Conchon, A., Titaud, O., Lehodey, P., 2020. Influence of oceanic conditions in the energy transfer efficiency estimation of a micronekton model. Biogeosciences 17, 833–850. https://doi.org/10.5194/bg-17-833-2020.

Drazen, J.C., Sutton, T.T., 2017. Dining in the Deep: The Feeding Ecology of Deep-Sea Fishes. Annu. Rev. Mar. Sci. 9, 337–366. https://doi.org/10.1146/annurev-marine-010816-060543.

Duffy, L.M., Kuhnert, P.M., Pethybridge, H.R., Young, J.W., Olson, R.J., Logan, J.M., Goñi, N., Romanov, E., Allain, V., Staudinger, M.D., Abecassis, M., Choy, C.A., Hobday, A.J., Simier, M., Galván-Magaña, F., Potier, M., Ménard, F., 2017. Global trophic ecology of yellowfin, bigeye, and albacore tunas: Understanding predation on micronekton communities at ocean-basin scales. Deep Sea Res. Part II Top. Stud. Oceanogr. 140, 55–73. https://doi.org/10.1016/j.dsr2.2017.03.003.

Dufresne, J.-L., Foujols, M.-A., Denvil, S., Caubel, A., Marti, O., Aumont, O., Balkanski, Y., Bekki, S., Bellenger, H., Benshila, R., Bony, S., Bopp, L., Braconnot, P., Brockmann, P., Cadule, P., Cheruy, F., Codron, F., Cozic, A., Cugnet, D., de Noblet, N., Duvel, J.-P., Ethé, C., Fairhead, L., Fichefet, T., Flavoni, S., Friedlingstein, P., Grandpeix, J.-Y., Guez, L., Guilyardi, E., Hauglustaine, D., Hourdin, F., Idelkadi, A., Ghattas, J., Joussaume, S., Kageyama, M., Krinner, G., Labetoulle, S., Lahellec, A., Lefebvre, M.-P., Lefevre, F., Levy, C., Li, Z.X., Lloyd, J., Lott, F., Madec, G., Mancip, M., Marchand, M., Masson, S., Meurdesoif, Y., Mignot, J., Musat, I., Parouty, S., Polcher, J., Rio, C., Schulz, M., Swingedouw, D., Szopa, S., Talandier, C., Terray, P., Viovy, N., Vuichard, N., 2013. Climate change projections using the IPSL-CM5 Earth System Model: from CMIP3 to CMIP5. Clim. Dyn. 40, 2123–2165. https://doi.org/10.1007/s00382-012-1636-1.

Dunne, J.P., John, J.G., Adcroft, A.J., Griffies, S.M., Hallberg, R.W., Shevliakova, E., Stouffer, R.J., Cooke, W., Dunne, K.A., Harrison, M.J., Krasting, J.P., Malyshev, S.L., Milly, P.C.D., Phillipps, P.J., Sentman, L.T., Samuels, B.L., Spelman, M.J., Winton, M., Wittenberg, A.T., Zadeh, N., 2012. GFDL's ESM2 Global Coupled Climate-Carbon Earth System Models. Part I: Physical Formulation and Baseline Simulation Characteristics. J. Clim. 25, 6646–6665. https://doi.org/10.1175/JCLI-D-11-00560.1.

Dussin, R., Barnier, B., Brodeau, L., Molines, J.M., 2016. The Making Of the DRAKKAR FORCING SET DFS5 (No. DRAKKAR/MyOcean Report 01–04-16).

Dutheil, C., Bador, M., Lengaigne, M., Lefevre, J., Jourdain, N.C., Vialard, J., Jullien, S., Peltier, A., Menkes, C., 2019. Impact of surface temperature biases on climate change projections of the South Pacific Convergence Zone. Clim. Dyn. Doi: 10.1007/s00382-019-04692-6.

Escobar-Flores, P., O'Driscoll, R., Montgomery, J., 2013. Acoustic characterization of pelagic fish distribution across the South Pacific Ocean. Mar. Ecol. Prog. Ser. 490, 169–183. https://doi.org/10.3354/meps10435.

Fu, W., Randerson, J.T., Moore, J.K., 2016. Climate change impacts on net primary production (NPP) and export production (EP) regulated by increasing stratification and phytoplankton community structure in the CMIP5 models. Biogeosciences 13, 5151–5170. https://doi.org/10.5194/bg-13-5151-2016.

Glover, A.G., Wiklund, H., Chen, C., Dahlgren, T.G., 2018. Managing a sustainable deep-sea 'blue economy' requires knowledge of what actually lives there. eLife 7. Doi: 10.7554/eLife.41319.

Gorgues, T., Aumont, O., Memery, L., 2019. Simulated Changes in the Particulate Carbon Export Efficiency due to Diel Vertical Migration of Zooplankton in the North Atlantic. Geophys. Res. Lett. 46, 5387–5395. https://doi.org/10.1029/2018GL081748.

Guinehut, S., Dhomps, A.-L., Larnicol, G., Le Traon, P.-Y., 2012. High Resolution 3-D temperature and salinity fields derived from in situ and satellite observations. Ocean Sci. Discuss. 9, 1313–1347. https://doi.org/10.5194/osd-9-1313-2012.

Handegard, N.O., du Buisson, L., Brehmer, P., Chalmers, S.J., De Robertis, A., Huse, G., Kloser, R., Macaulay, G., Maury, O., Ressler, P.H., Stenseth, N.C., Godø, O.R., 2013. Towards an acoustic-based coupled observation and modelling system for monitoring and predicting ecosystem dynamics of the open ocean. Fish Fish. 14, 605–615. https://doi.org/10.1111/j.1467-2979.2012.00480.x.

Hidalgo, M., Browman, H.I., 2019. Developing the knowledge base needed to sustainably manage mesopelagic resources. ICES J. Mar. Sci. 76, 609–615. https://doi.org/10.1093/icesjms/fsz067.

Hillebrand, H., Brey, T., Gutt, J., Hagen, W., Metfies, K., Meyer, B., Lewandowska, A., 2018. Climate Change: Warming Impacts on Marine Biodiversity, in: Salomon, M., Markus, T. (Eds.), Handbook on Marine Environment Protection : Science, Impacts and Sustainable Management. Springer International Publishing, Cham, pp. 353–373. Doi: 10.1007/978-3-319-60156-4_18.

Irigoien, X., Klevjer, T.A., Røstad, A., Martinez, U., Boyra, G., Acuña, J.L., Bode, A., Echevarria, F., Gonzalez-Gordillo, J.I., Hernandez-Leon, S., Agusti, S., Aksnes, D.L., Duarte, C.M., Kaartvedt, S., 2014. Large mesopelagic fishes biomass and trophic efficiency in the open ocean. Nat. Commun. 5 https://doi.org/10.1038/ncomms4271.

Johnson, J., Allain, V., johann, B., Lehodey, P., Nicol, S., Senina, I., 2018. Effects of Climate Change on Ocean Fisheries Relevant to the Pacific Islands. Pac. Mar. Clim. CHANGE Rep. CARD 177–188.

Klevjer, T.A., Irigoien, X., Røstad, A., Fraile-Nuez, E., Benítez-Barrios, V.M., Kaartvedt, S., 2016. Large scale patterns in vertical distribution and behaviour of mesopelagic scattering layers. Sci. Rep. 6, 19873. https://doi.org/10.1038/srep19873.

Knutson, T.R., Sirutis, J.J., Garner, S.T., Vecchi, G.A., Held, I.M., 2008. Simulated reduction in Atlantic hurricane frequency under twenty-first-century warming conditions. Nat. Geosci. 1, 359–364. https://doi.org/10.1038/ngeo202.

Kuhn, M., Wing, J., Weston, S., Williams, A., Keefer, C., Engelhardt, A., Cooper, T., Mayer, Z., Kenkel, B., R Core Team, Benesty, M., Lescarbeau, R., Ziem, A., Scrucca, L., Tang, Y., Candan, C., Hunt, T., 2020. caret: Classification and Regression Training.

Kwiatkowski, L., Aumont, O., Bopp, L., 2019. Consistent trophic amplification of marine biomass declines under climate change. Glob. Change Biol. 25, 218–229. https://doi.org/10.1111/gcb.14468.

Kwiatkowski, L., Bopp, L., Aumont, O., Ciais, P., Cox, P.M., Laufkötter, C., Li, Y., Séférian, R., 2017. Emergent constraints on projections of declining primary production in the tropical oceans | Nature Climate Change. Nat. Clim. Change 7. https://doi.org/10.1038/NCLIMATE3265.

Lambert, C., Mannocci, L., Lehodey, P., Ridoux, V., 2014. Predicting Cetacean Habitats from Their Energetic Needs and the Distribution of Their Prey in Two Contrasted Tropical Regions. PLOS ONE 9, e105958. https://doi.org/10.1371/journal.pone.0105958.

Laufkötter, C., Vogt, M., Gruber, N., Aita-noguchi, M., Aumont, O., Bopp, L., Buitenhuis, E., Doney, S.C., Dunne, J., Hashioka, T., Hauck, J., Hirata, T., John, J., Le Quéré, C., Lima, I.D., Nakano, H., Seferian, R., Totterdell, I., Vichi, M., Völker, C., 2015. Drivers and uncertainties of future global marine primary production in marine ecosystem models. Biogeosciences 12, 6955–6984. https://doi.org/10.5194/bg-12-6955-2015.

Le Borgne, R., Allain, V., Griffiths, S.P., Matear, R.J., McKinnon, A.D., Richardson, A.J., Young, J.W., 2011. Vulnerability of open ocean food webs in the tropical Pacific to climate change, in: Vulnerability of Tropical Pacific Fisheries and Aquaculture to Climate Change. Secretariat of the Pacific Community, New Caledonia.

Lefort, S., Aumont, O., Bopp, L., Arsouze, T., Gehlen, M., Maury, O., 2015. Spatial and body-size dependent response of marine pelagic communities to projected global climate change. Glob. Change Biol. 21, 154–164. https://doi.org/10.1111/gcb.12679.

Lehodey, P., Conchon, A., Senina, I., Domokos, R., Calmettes, B., Jouanno, J., Hernandez, O., Kloser, R., 2015a. Optimization of a micronekton model with acoustic data. ICES J. Mar. Sci. 72, 1399–1412. https://doi.org/10.1093/icesjms/fsu233.

Lehodey, Patrick, Murtugudde, R., Senina, I., 2010a. Bridging the gap from ocean models to population dynamics of large marine predators: A model of mid-trophic functional groups. Prog. Oceanogr. 84, 69–84. https://doi.org/10.1016/j.pocean.2009.09.008.

Lehodey, P., Senina, I., Calmettes, B., Hampton, J., Nicol, S., 2013. Modelling the impact of climate change on Pacific skipjack tuna population and fisheries. Clim. Change 119, 95–109. https://doi.org/10.1007/s10584-012-0595-1.

Lehodey, Patrick, Senina, I., Nicol, S., Hampton, J., 2015b. Modelling the impact of climate change on south pacific albacore tuna. Deep-Sea Res. Part II Top. Stud. Oceanogr. 113, 246–259. https://doi.org/10.1016/j.dsr2.2014.10.028.

Lehodey, P., Senina, I., Sibert, J., Bopp, L., Calmettes, B., Hampton, J., Murtugudde, R., 2010b. Preliminary forecasts of Pacific bigeye tuna population trends under the A2 IPCC scenario. Prog. Oceanogr. 86, 302–315. https://doi.org/10.1016/j.pocean.2010.04.021.

Lehodey, P., Senina, I., Sibert, J., Hampton, J., 2008. SEAPODYM v2: a spatial ecosystem and population dynamics model with parameter optimization providing a new tool for tuna management. Scientific Committee Fourth Regular Session, Port Moresby, Papua New Guinea.

Li, G., Du, Y., Xu, H., Ren, B., 2015. An Intermodel Approach to Identify the Source of Excessive Equatorial Pacific Cold Tongue in CMIP5 Models and Uncertainty in Observational Datasets. J. Clim. 28, 7630–7640. https://doi.org/10.1175/JCLI-D-15-0168.1.

Li, G., Xie, S.-P., Du, Y., Luo, Y., 2016. Effects of excessive equatorial cold tongue bias on the projections of tropical Pacific climate change. Part I: the warming pattern in

CMIP5 multi-model ensemble. Clim. Dyn. 47, 3817–3831. https://doi.org/10.1007/s00382-016-3043-5.
Longhurst, A.R., 2007. Ecological geography of the sea. Academic Press, Amsterdam, Boston, MA.
Lotze, H.K., Tittensor, D.P., Bryndum-Buchholz, A., Eddy, T.D., Cheung, W.W.L., Galbraith, E.D., Barange, M., Barrier, N., Bianchi, D., Blanchard, J.L., Bopp, L., Büchner, M., Bulman, C.M., Carozza, D.A., Christensen, V., Coll, M., Dunne, J.P., Fulton, E.A., Jennings, S., Jones, M.C., Mackinson, S., Maury, O., Niiranen, S., Oliveros-Ramos, R., Roy, T., Fernandes, J.A., Schewe, J., Shin, Y.-J., Silva, T.A.M., Steenbeek, J., Stock, C.A., Verley, P., Volkholz, J., Walker, N.D., Worm, B., 2019. Global ensemble projections reveal trophic amplification of ocean biomass declines with climate change. Proc. Natl. Acad. Sci. 116, 12907–12912. https://doi.org/10.1073/pnas.1900194116.
MacLennan, D.N., 2002. A consistent approach to definitions and symbols in fisheries acoustics. ICES J. Mar. Sci. 59, 365–369. https://doi.org/10.1006/jmsc.2001.1158.
Madec, G., NEMO team, 2008. NEMO ocean engine (Note du Pole de mod ˆelisation de l'Institut Pierre-Simon Laplace No 27́ No. 27). Institut Pierre-Simon Laplace (IPSL).
Mannocci, L., Laran, S., Monestiez, P., Dorémus, G., Van Canneyt, O., Watremez, P., Ridoux, V., 2014. Predicting top predator habitats in the Southwest Indian Ocean. Ecography 37, 261–278. https://doi.org/10.1111/j.1600-0587.2013.00317.x.
Matear, R.J., Chamberlain, M.A., Sun, C., Feng, M., 2015. Climate change projection for the western tropical Pacific Ocean using a high-resolution ocean model: Implications for tuna fisheries. Deep Sea Res. Part II Top. Stud. Oceanogr Impacts Climate Marine top predators 113, 22–46. https://doi.org/10.1016/j.dsr2.2014.07.003.
Menkes, C.E., Allain, V., Rodier, M., Gallois, F., Lebourges-Dhaussy, A., Hunt, B.P.V., Smeti, H., Pagano, M., Josse, E., Daroux, A., Lehodey, P., Senina, I., Kestenare, E., Lorrain, A., Nicol, S., 2015. Seasonal oceanography from physics to micronekton in the south-west Pacific. Deep Sea Res. Part II Top. Stud. Oceanogr. 113, 125–144. https://doi.org/10.1016/j.dsr2.2014.10.026.
Miller, M.G.R., Carlile, N., Phillips, J.S., McDuie, F., Congdon, B.C., 2018. Importance of tropical tuna for seabird foraging over a marine productivity gradient. Mar. Ecol. Prog. Ser. 586, 233–249. https://doi.org/10.3354/meps12376.
Moore, J.K., Fu, W., Primeau, F., Britten, G.L., Lindsay, K., Long, M., Doney, S.C., Mahowald, N., Hoffman, F., Randerson, J.T., 2018. Sustained climate warming drives declining marine biological productivity. Science 359, 1139–1143. https://doi.org/10.1126/science.aao6379.
Olivar, M.P., Hulley, P.A., Castellón, A., Emelianov, M., López, C., Tuset, V.M., Contreras, T., Molí, B., 2017. Mesopelagic fishes across the tropical and equatorial Atlantic: Biogeographical and vertical patterns. Prog. Oceanogr. 151, 116–137. https://doi.org/10.1016/j.pocean.2016.12.001.
Olson, R., Duffy, L., Kuhnert, P., Galván-Magaña, F., Bocanegra-Castillo, N., Alatorre-Ramírez, V., 2014. Decadal diet shift in yellowfin tuna Thunnus albacares suggests broad-scale food web changes in the eastern tropical Pacific Ocean. Mar. Ecol. Prog. Ser. 497, 157–178. https://doi.org/10.3354/meps10609.
Parmesan, C., 2006. Ecological and Evolutionary Responses to Recent Climate Change. Annu. Rev. Ecol. Evol. Syst. 37, 637–669. https://doi.org/10.1146/annurev.ecolsys.37.091305.110100.
Payne, M.R., Barange, M., Cheung, W.W.L., MacKenzie, B.R., Batchelder, H.P., Cormon, X., Eddy, T.D., Fernandes, J.A., Hollowed, A.B., Jones, M.C., Link, J.S., Neubauer, P., Ortiz, I., Queirós, A.M., Paula, J.R., 2016. Uncertainties in projecting climate-change impacts in marine ecosystems. ICES J. Mar. Sci. 73, 1272–1282. https://doi.org/10.1093/icesjms/fsv231.
Payri, C.E., Allain, V., Aucan, J., David, C., David, V., Dutheil, C., Loubersac, L., Menkes, C., Pelletier, B., Pestana, G., Samadi, S., 2019. Chapter 27 - New Caledonia, in: Sheppard, C. (Ed.), World Seas: An Environmental Evaluation (Second Edition). Academic Press, pp. 593–618. Doi: 10.1016/B978-0-08-100853-9.00035-X.
Pecl, G.T., Araújo, M.B., Bell, J.D., Blanchard, J., Bonebrake, T.C., Chen, I.-C., Clark, T. D., Colwell, R.K., Danielsen, F., Evengård, B., Falconi, L., Ferrier, S., Frusher, S., Garcia, R.A., Griffis, R.B., Hobday, A.J., Janion-Scheepers, C., Jarzyna, M.A., Jennings, S., Lenoir, J., Linnetved, H.I., Martin, V.Y., McCormack, P.C., McDonald, J., Mitchell, N.J., Mustonen, T., Pandolfi, J.M., Pettorelli, N., Popova, E., Robinson, S.A., Scheffers, B.R., Shaw, J.D., Sorte, C.J.B., Strugnell, J.M., Sunday, J. M., Tuanmu, M.-N., Vergés, A., Villanueva, C., Wernberg, T., Wapstra, E., Williams, S.E., 2017. Biodiversity redistribution under climate change: Impacts on ecosystems and human well-being. Science 355, eaai9214. https://doi.org/10.1126/science.aai9214.
Pörtner, H., 2001. Climate change and temperature-dependent biogeography: oxygen limitation of thermal tolerance in animals. Naturwissenschaften 88, 137–146. https://doi.org/10.1007/s001140100216.
Proud, R., Cox, M.J., Brierley, A.S., 2017. Biogeography of the Global Ocean's Mesopelagic Zone. Curr. Biol. 27, 113–119. https://doi.org/10.1016/j.cub.2016.11.003.
Proud, R., Handegard, N.O., Kloser, R.J., Cox, M.J., Brierley, A.S., Handling editor: David Demer, 2018. From siphonophores to deep scattering layers: uncertainty ranges for the estimation of global mesopelagic fish biomass. ICES J. Mar. Sci. Doi: 10.1093/icesjms/fsy037.
Receveur, A., Kestenare, E., Allain, V., Menard, F., Cravatte, S., Lebourges-Dhaussy, A., Lehodey, P., Mangeas, M., Smith, N., Radenac, M.H., Menkes, C., 2020a. Micronekton distribution in the southwest Pacific (New Caledonia) inferred from Shipboard-ADCP backscatter data. Deep.
Receveur, A., Menkes, C., Allain, V., Lebourges-Dhaussy, A., Nerini, D., Mangeas, M., Menard, F., 2019. Seasonal and spatial variability in the vertical distribution of pelagic forage fauna in the southwest Pacific. Deep Sea Res. Part II. Doi: 10.1016/j.dsr2.2019.104655.
Receveur, A., Vourey, E., Lebourges Dhaussy, A., Menkes, C., Menard, F., Allain, V., 2020b. Biogeography of micronekton assemblages in the Natural Park of the Coral Sea. Front. Mar. Sci. 7 https://doi.org/10.3389/fmars.2020.00449.
Ridgway, K.R., Dunn, J.R., Wilkin, J.L., 2002. Ocean Interpolation by Four-Dimensional Weighted Least Squares—Application to the Waters around Australasia. J. Atmospheric Ocean. Technol. 19, 1357–1375. https://doi.org/10.1175/1520-0426(2002)019<1357:OIBFDW>2.0.CO;2.
Saulquin, B., Gohin, F., Garello, R., 2009. Regional objective analysis for merging MERIS, MODIS/Aqua and SeaWiFS Chlorophyll-a data from 1998 to 2008 on the European Atlantic Shelf at a resolution of 1.1Km. Oceans 2009 - Eur. 1, 1165–1174. Doi: 10.1109/OCEANSE.2009.5278165.
Senina, I., Lehodey, P., Calmettesa, B., Nicol, S., Caillot, S., Hampton, J., Williams, P., 2016. Predicting skipjack tuna dynamics and effects of climate change using SEAPODYM with fishing and tagging data. SC12 EB-WP-01. Twelfth Regular Session of the Scientific Committee of the WCPFC. Bali, Indonesia. 3–11 August.
St. John, M.A., Borja, A., Chust, G., Heath, M., Grigorov, I., Mariani, P., Martin, A.P., Santos, R.S., 2016. A Dark Hole in Our Understanding of Marine Ecosystems and Their Services: Perspectives from the Mesopelagic Community. Front. Mar. Sci. 3. Doi: 10.3389/fmars.2016.00031.
Taylor, K.E., Stouffer, R.J., Meehl, G.A., 2012. An Overview of CMIP5 and the Experiment Design. Bull. Am. Meteorol. Soc. 93, 485–498. https://doi.org/10.1175/BAMS-D-11-00094.1.
van Vuuren, D.P., Edmonds, J., Kainuma, M., Riahi, K., Thomson, A., Hibbard, K., Hurtt, G.C., Kram, T., Krey, V., Lamarque, J.-F., Masui, T., Meinshausen, M., Nakicenovic, N., Smith, S.J., Rose, S.K., 2011. The representative concentration pathways: an overview. Clim. Change 109, 5. https://doi.org/10.1007/s10584-011-0148-z.
Wang, C., Zhang, L., Lee, S.-K., Wu, L., Mechoso, C.R., 2014. A global perspective on CMIP5 climate model biases. Nat. Clim. Change 4, 201–205. https://doi.org/10.1038/nclimate2118.
Watanabe, S., Hajima, T., Sudo, K., Nagashima, T., Takemura, T., Okajima, H., Nozawa, T., Kawase, H., Abe, M., Yokohata, T., Ise, T., Sato, H., Kato, E., Takata, K., Emori, S., Kawamiya, M., 2011. MIROC-ESM 2010: model description and basic results of CMIP5-20c3m experiments. Geosci. Model Dev. 4, 845–872. https://doi.org/10.5194/gmd-4-845-2011.
Weimerskirch, H., Borsa, P., Cruz, S., de Grissac, S., Gardes, L., Lallemand, J., Le Corre, M., Prudor, A., 2017. Diversity of migration strategies among great frigatebirds populations. J. Avian Biol. 48, 103–113. https://doi.org/10.1111/jav.01330.
Wentz, F.J., Scott, R.H., Leidner, M., Atlas, R., Ardizzone, J., 2015. Remote Sensing Systems Cross-Calibrated Multi-Platform (CCMP) 6-hourly ocean vector wind analysis product on 0.25 deg grid, Remote Sensing Systems. Santa Rosa, CA.
Williams, A.J., Allain, V., Nicol, S.J., Evans, K.J., Hoyle, S.D., Dupoux, C., Vourey, E., Dubosc, J., 2014. Vertical behavior and diet of albacore tuna (Thunnus alalunga) vary with latitude in the South Pacific Ocean. Deep Sea Res. Part II.
Xie, S.-P., Deser, C., Vecchi, G.A., Collins, M., Delworth, T.L., Hall, A., Hawkins, E., Johnson, N.C., Cassou, C., Giannini, A., Watanabe, M., 2015. Towards predictive understanding of regional climate change. Nat. Clim. Change 5, 921–930. https://doi.org/10.1038/nclimate2689.
Young, J.W., Lansdell, M.J., Campbell, R.A., Cooper, S.P., Juanes, F., Guest, M.A., 2010. Feeding ecology and niche segregation in oceanic top predators off eastern Australia. Mar. Biol. 157, 2347–2368. https://doi.org/10.1007/s00227-010-1500-y.